Neuron
Article

Linking Cell Fate, Trajectory Choice, and Target Selection: Genetic Analysis of Sema-2b in Olfactory Axon Targeting

William J. Joo,[1,2] Lora B. Sweeney,[1,2,4] Liang Liang,[1,3] and Liqun Luo[1,2,*]
[1]Howard Hughes Medical Institute and Department of Biology
[2]Neurosciences Graduate Program
[3]Applied Physics Graduate Program
Stanford University, Stanford, CA 94305, USA
[4]Present address: Salk Institute for Biological Studies, La Jolla, CA 92037, USA
*Correspondence: lluo@stanford.edu
http://dx.doi.org/10.1016/j.neuron.2013.03.022

SUMMARY

Neural circuit assembly requires selection of specific cell fates, axonal trajectories, and synaptic targets. By analyzing the function of a secreted semaphorin, Sema-2b, in *Drosophila* olfactory receptor neuron (ORN) development, we identified multiple molecular and cellular mechanisms that link these events. Notch signaling limits Sema-2b expression to ventromedial ORN classes, within which Sema-2b cell-autonomously sensitizes ORN axons to external semaphorins. Central-brain-derived Sema-2a and Sema-2b attract Sema-2b-expressing axons to the ventromedial trajectory. In addition, Sema-2b/PlexB-mediated axon-axon interactions consolidate this trajectory choice and promote ventromedial axon-bundle formation. Selecting the correct developmental trajectory is ultimately essential for proper target choice. These findings demonstrate that Sema-2b couples ORN axon guidance to postsynaptic target neuron dendrite patterning well before the final target selection phase, and exemplify how a single guidance molecule can drive consecutive stages of neural circuit assembly with the help of sophisticated spatial and temporal regulation.

INTRODUCTION

Neural circuit assembly relies on the coordinated efforts of diverse developmental processes. Neurons must first acquire distinct fates, which eventually determine their wiring specificity and physiological properties. Axons then navigate along specific pathways toward their target cells, often across long distances. Finally, axons choose specific synaptic partners within the target zone. While significant progress has been made during the past few decades in our understanding of each of these steps (reviewed in Sanes and Yamagata, 2009; Jukam and Desplan, 2010; Kolodkin and Tessier-Lavigne, 2011), less is known about the cellular and molecular mechanisms that seamlessly coordinate such distinct developmental processes.

The olfactory system relies on highly organized inputs from diverse olfactory receptor neuron (ORN) classes and thus offers an excellent context in which to explore the relationships between cell fate, axon pathway choice, and target selection. In *Drosophila*, 50 classes of ORNs, most of which express a single odorant receptor, target their axons precisely to 50 corresponding glomeruli in the antennal lobe (Couto et al., 2005; Fishilevich and Vosshall, 2005; Silbering et al., 2011). ORN axons synapse on projection neuron (PN) dendrites, most of which arborize within a single glomerulus (Stocker et al., 1990; Jefferis et al., 2001). Thus, a key feature in the olfactory circuit is the precise establishment of one-to-one pairs between 50 ORN classes and 50 PN classes. PN dendrites pattern the developing antennal lobe first. By 18 hr after puparium formation (APF), when pioneering ORN axons reach the developing antennal lobe, dendrites of individual PNs already occupy specific areas within the antennal lobe corresponding to their future glomerular positions (Jefferis et al., 2004). The secreted semaphorins Sema-2a and Sema-2b are expressed in a gradient within the antennal lobe and signal through transmembrane Sema-1a to instruct PN dendrite targeting along the dorsolateral-ventromedial axis (Komiyama et al., 2007; Sweeney et al., 2011). Local binary determinants such as Capricious further segregate PN dendrites into discrete glomeruli (Hong et al., 2009). Several distinct mechanisms of ORN axon targeting have also been identified. For example, Sema-1a also mediates repulsive axon-axon interactions to segregate ORN axons from different sensory organs (Lattemann et al., 2007; Sweeney et al., 2007). Hedgehog signaling coordinates peripheral ORN cell body position with antennal lobe glomerular targeting (Chou et al., 2010). Teneurin-mediated homophilic attraction matches PN dendrites with corresponding ORN axons during final target selection (Hong et al., 2012). With the exception of Teneurin-mediated synaptic partner matching, it remains unclear how and when axon-derived and target-derived cues cooperate, or how the development of PN dendrites and ORN axons is coordinated.

ORNs expressing a specific odorant receptor exhibit characteristic olfactory responses (Hallem and Carlson, 2006), which are sent to particular glomeruli and relayed by postsynaptic

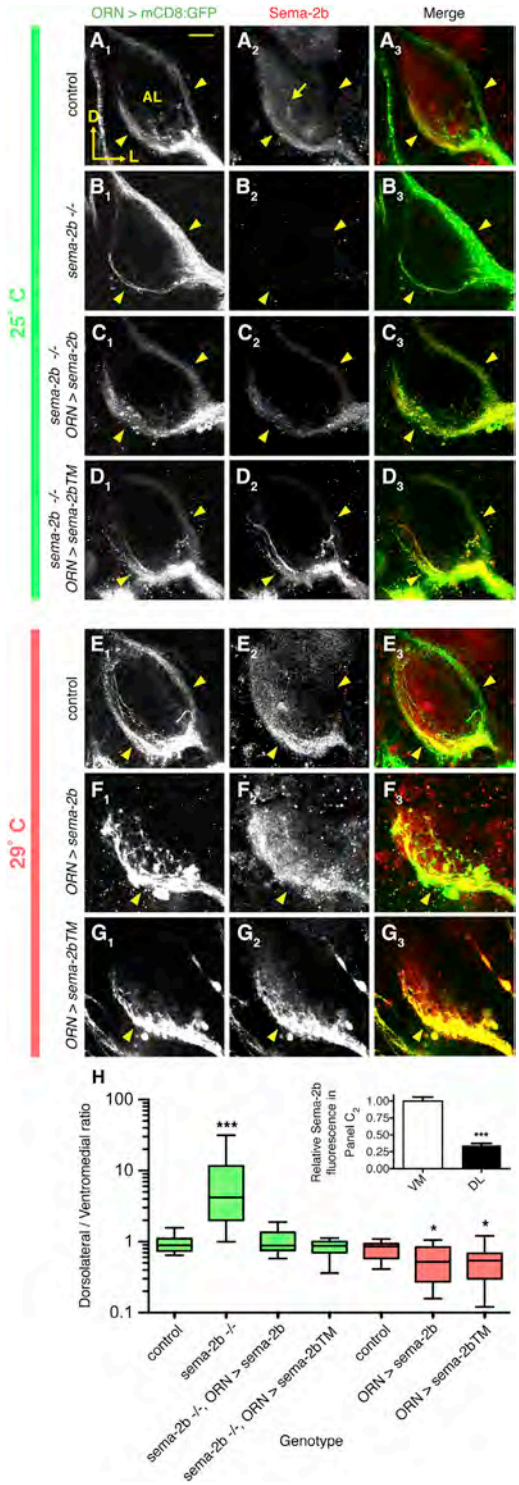

Figure 1. Sema-2b Is Selectively Expressed in Ventromedial ORNs and Specifies Their Axon Trajectories

(A_1–A_3) (A_1) Developing ORN axons choose either a ventromedial or dorsolateral trajectory (yellow arrowheads) as they circumnavigate the antennal lobe (AL) at 24 hr APF; all ORN axons are labeled by *pebbled-GAL4* driving *UAS-mCD8:GFP*. (A_2) Only ventromedial axons express high levels of Sema-2b protein. Sema-2b is also enriched within the ventromedial antennal lobe (arrow). (A_3) Merge of A_1 and A_2. D, dorsal; L, lateral. Midline is to the left. Scale bar = 10 μm for all images of pupal brains.

(B) In *sema-2b*$^{-/-}$ mutants, ORN axons primarily take the dorsolateral trajectory; the ventromedial axon bundle is markedly reduced. The absence of Sema-2b staining in *sema-2b* mutant (B_2) confirms antibody specificity.

(C and D) ORN-specific expression of *UAS-sema-2b* (C) or *UAS-sema-2b*^{TM} (D) rescues ventromedial axon trajectory in *sema-2b*$^{-/-}$ mutants.

(E–G) At 29°C, ORN-specific overexpression of secreted (F) or membrane-tethered (G) Sema-2b in a wild-type background causes more axons to choose the ventromedial trajectory compared to control (E).

(H) Quantification of dorsolateral/ventromedial axon bundle ratio. See Supplemental Experimental Procedures for details. Boxes indicate geometric mean (middle line) and 25%–75% range, while whiskers indicate maximum and minimum values. Geometric means/sample sizes are as follows: 25°C control, 0.90/16; *sema-2b*$^{-/-}$, 4.77/33; *sema-2b*$^{-/-}$, *ORN > sema-2b*, 0.97/14; *sema-2b*$^{-/-}$, *ORN > sema-2b*^{TM}, 0.81/27; 29°C control, 0.74/16; *ORN > sema-2b*, 0.45/24; *ORN > sema-2b*^{TM}, 0.46/25. (Inset) Quantification of pan ORN > Sema-2b overexpression levels (in a *sema2b*$^{-/-}$ background) in ventromedial (VM) versus dorsolateral (DL) axon bundles for Figure 1C. Sema-2b fluorescence intensity was normalized to mCD8:GFP fluorescence. ***$p < 0.001$; *$p < 0.05$, one-way ANOVA with Bonferroni's multiple comparison test.

target PNs to stereotyped areas in higher olfactory centers (Jefferis et al., 2007). ORNs are housed in specific sensilla in the 3rd segment of the antennae and in the maxillary palps. Most sensilla contain two to three individual ORNs belonging to distinct classes. The Notch pathway diversifies ORN fates within individual sensilla (Endo et al., 2007). Loss of *mastermind* (*mam*), a transcriptional coactivator that mediates Notch signaling, causes ORNs to adopt a "Notch-OFF" fate, whereas loss of *numb,* an antagonist of Notch signaling, causes ORNs to adopt a "Notch-ON" fate. Notch-OFF and Notch-ON ORN classes target their axons to distinct glomeruli. However, the specific molecules and mechanisms that mediate such targeting are currently unknown. By analyzing Sema-2b function in ORN axon targeting, we now report molecular and cellular mechanisms that link ORN cell fate, trajectory choice, and target selection. Our findings also demonstrate that Sema-2b couples PN dendrite patterning with ORN axon guidance well before the final target selection phase, thus newly connecting previously disparate steps in olfactory circuit wiring.

RESULTS

Sema-2b Is Selectively Expressed by the Ventromedial ORN Axon Bundle

While examining the role of secreted semaphorins in PN dendrite targeting (Sweeney et al., 2011), we observed a striking distribution pattern for Sema-2b in adult ORNs. Pioneering antennal ORN axons first contact the ventrolateral edge of the developing antennal lobe at 18 hr APF (Jefferis et al., 2004). They then circumscribe the ipsilateral antennal lobe and navigate across the midline before invading both the ipsi- and contralateral antennal lobes. At 24 hr APF, ORN axons labeled with the pan-ORN *pebbled-GAL4* driver (Sweeney et al., 2007) took either a ventromedial or dorsolateral trajectory around the antennal lobe (Figure 1A_1). ORN axons thus segregated into two distinct bundles of roughly equal size, with a mean dorsolateral/ventromedial ratio of 0.90 (Figure 1H). Notably, Sema-2b protein was highly enriched in the ventromedial axon bundle but was

undetectable from the dorsolateral bundle (Figure 1A$_2$). It was also present within the ventromedial antennal lobe (Figure 1A$_2$, arrow) where it is contributed by a central source (Sweeney et al., 2011). Based on this highly specific distribution pattern, we hypothesized that Sema-2b plays a crucial role in ORN axon trajectory choice.

Sema-2b Acts in ORNs to Specify Ventromedial Trajectory Choice

Indeed, in 24-hr-APF *sema-2b* homozygous mutant (*sema-2b*$^{-/-}$) brains, the dorsolateral axon bundle was enlarged at the expense of the ventromedial bundle, shifting the average dorsolateral/ventromedial ratio to 4.77 (Figures 1B and 1H). Sema-2b is thus required for ventromedial trajectory choice. Given that both the central brain and peripheral ventromedial ORNs contribute Sema-2b (Figure 1A$_2$), we next tested its cell-type-specific function by using *pebbled-GAL4* to drive *UAS-sema-2b* expression in *sema-2b*$^{-/-}$ mutants. This restored the ventromedial axon bundle size to wild-type (WT) levels (Figures 1C and 1H; mean ratio = 0.97), demonstrating that ORN-derived Sema-2b alone is sufficient to rescue the ventromedial axon trajectory defects of *sema-2b*$^{-/-}$ mutants in the absence of central Sema-2b. A membrane-tethered version of Sema-2b (Sema-2b^{TM}; Wu et al., 2011) also rescued trajectory with similar efficiency (Figures 1D and 1H; mean ratio = 0.81), suggesting that secretion is not obligatory for Sema-2b function. Sema-2b thus acts locally at the membrane rather than as a long-distance secreted cue.

While pan-ORN Sema-2b expression restored the dorsolateral/ventromedial axon bundle ratio, we observed that Sema-2b protein was not expressed equally between the two bundles, with 3-fold lower expression in the dorsolateral bundle relative to the ventromedial bundle (Figure 1C$_2$; quantified in Figure 1H, inset). This may have facilitated rescue, and suggests that endogenous posttranscriptional mechanisms downregulate Sema-2b in dorsolateral ORNs (see Discussion).

We further tested whether ORN-specific Sema-2b overexpression could redirect dorsolateral axons to the ventromedial trajectory. Because overexpression at 25°C did not cause significant phenotypes (data not shown), likely due to the posttranscriptional downregulation in dorsolateral ORNs, we raised experimental flies at 29°C to increase *UAS-Sema-2b* transcription levels. Under these conditions, both secreted and membrane-tethered Sema-2b biased axons toward the ventromedial trajectory, in some cases almost completely removing the dorsolateral bundle (mean dorsolateral/ventromedial ratio = 0.45 and 0.46 for secreted and membrane-tethered Sema-2b, respectively). Sufficiently high levels of Sema-2b can thus force dorsolateral axons to choose the ventromedial trajectory. Taken together, our expression and loss- and gain-of-function studies indicate that Sema-2b is required in ventromedial ORNs for proper trajectory choice and plays an instructive role in specifying ventromedial trajectory choice.

Glomerular Targeting Is Differentially Affected in *sema-2b* Mutants Based on ORN Class

What are the consequences of incorrect trajectory choice for ORN class-specific glomerular targeting? To systematically examine this question, we labeled individual ORN classes in the adult brain with odorant receptor (Or) promoter-driven GAL4 lines. In WT, *Or92a-GAL4* and *Or67b-GAL4* each label a "ventromedial" ORN class that sends its axons along a ventromedial trajectory and targets to the VA2 and VA3 glomeruli in the ventromedial antennal lobe, respectively (Figure 2A, top row). In *sema-2b*$^{-/-}$ brains, the majority of axons for both ORN classes took dorsolateral trajectories around the antennal lobe and terminated in specific ectopic loci in the dorsolateral antennal lobe (Figure 2A, bottom row). Residual axons that took the ventromedial trajectory terminated in approximately correct target regions.

In contrast to the severe phenotypes of ventromedial classes, "dorsolateral" ORN classes exhibited little or no trajectory and targeting defects: both *Or67d-GAL4* and *Or88a-GAL4* label dorsolaterally projecting ORN classes that target to the DA1 and VA1d glomeruli, respectively. Neither class was affected in *sema-2b* mutants (Figure 2B), consistent with the absence of Sema-2b expression in the dorsolateral-targeting ORNs during development (Figure 1).

In a third group of ORN classes exemplified by Or22a and Or47a, axons normally choose ventromedial trajectories and target to dorsomedial glomeruli (Figure 2C). Interestingly, their trajectories were severely affected in *sema-2b*$^{-/-}$ brains, just as in ventromedial classes, but their glomerular targeting remained largely normal. Glomerular targeting of dorsomedial ORN classes can thus be independent of trajectory choice.

To extend these results more globally, we analyzed 19 additional ORN classes, all of which reinforced the class-specific *sema-2b*$^{-/-}$ phenotypes described above (Figure S1 available online). Altogether, 10 different ventromedial classes exhibited severe and highly penetrant trajectory and targeting phenotypes (red, Figures 2D and 2E; Figure S1A), while eight dorsolateral classes were mostly unaffected and six dorsomedial classes exhibited severe trajectory-choice phenotypes with only mild targeting defects (blue and orange, Figures 2D and 2E; Figures S1B and S1C). Furthermore, ORN-specific removal of *sema-2b* using eyFlp-driven mosaic analysis with a repressible cell marker (MARCM; Lee and Luo, 1999; Figure S2C) caused targeting and trajectory phenotypes nearly identical to those of whole-animal homozygous mutants, both qualitatively and quantitatively (Figure S2). This demonstrates further that Sema-2b is required in ORNs for axon trajectory and glomerular targeting.

In summary, axon-trajectory phenotypes of *sema-2b*$^{-/-}$ mutants have class-specific consequences for final target selection. For dorsolateral ORN classes, glomerular targeting is normal since Sema-2b was not required for their trajectory choice (Figure 2E, middle). For dorsomedial classes, initial axon trajectory choice is incorrect, but glomerular targeting is minimally affected, because target glomeruli are close to the midline commissure region where axons from ventromedial and dorsolateral trajectories reconvene (Figure 2E, right). For ventromedial ORNs, incorrect trajectory choice has devastating consequences for targeting; axons that aberrantly choose dorsolateral trajectories cannot take alternate routes to their targets but instead terminate in the dorsolateral antennal lobe far away from their normal targets (Figure 2E, left).

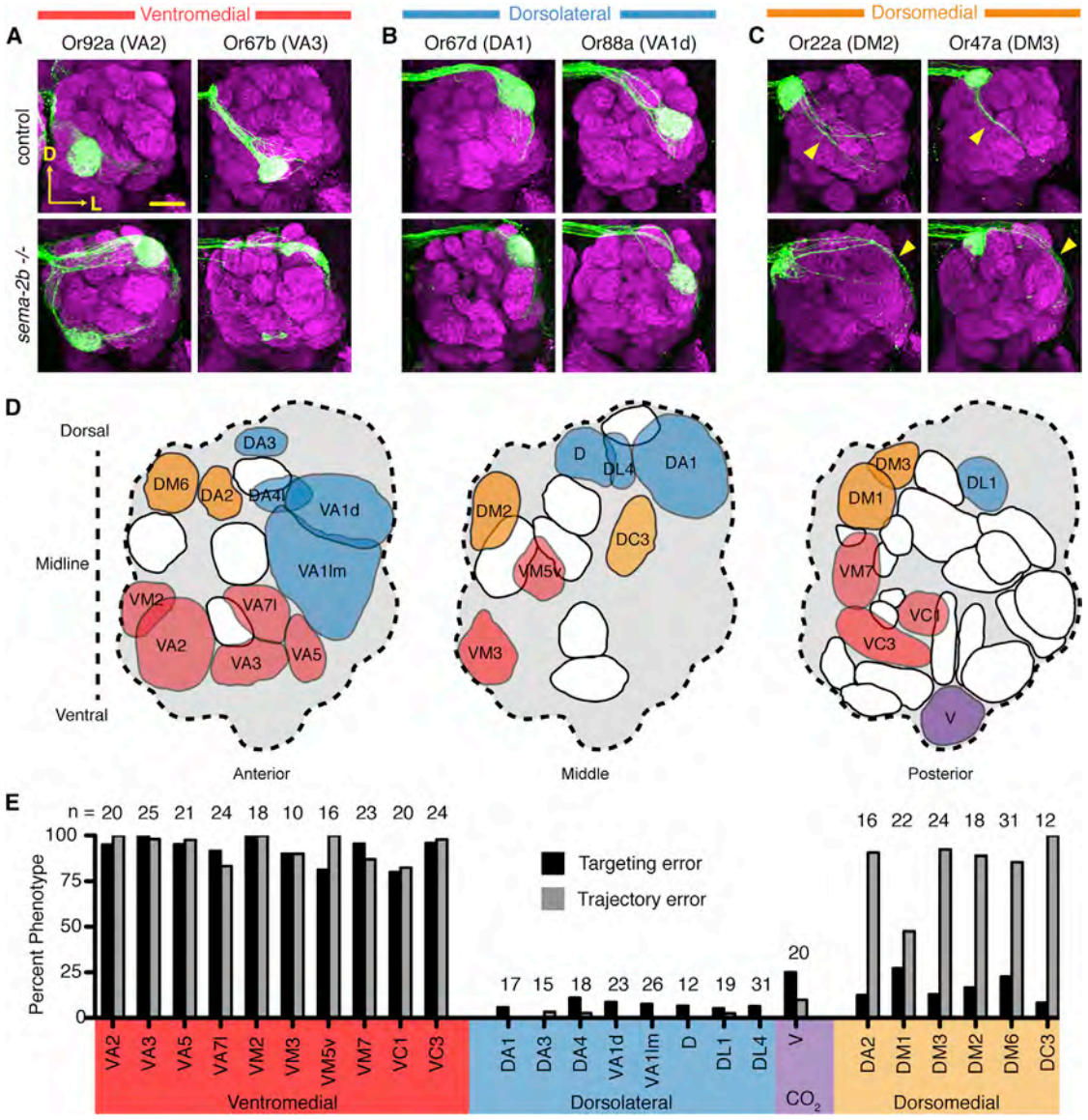

Figure 2. Sema-2b Is Required for Trajectory Choice and Glomerular Target Selection of Ventromedial ORNs

(A–C) Glomerular targeting of axons (labeled in green) from specific ORN classes in control (top) or *sema-2b*$^{-/-}$ mutant (bottom) adult brains. nc82 staining labels the antennal lobe neuropil (magenta). ORN classes and their glomerular targets (in parentheses) are indicated above the images. D, dorsal; L, lateral. Scale bar = 20 μm (for all adult brain images). Axons of the "ventromedial" ORN classes Or92a and Or67b (A) normally take ventromedial trajectories to target the VA2 and VA3 glomeruli, respectively. In *sema-2b*$^{-/-}$ mutant brains, the majority of axons aberrantly project dorsolaterally to incorrect targets. Axons of the "dorsolateral" classes Or67d and Or88a (B) normally target DA1 and VA1d, respectively; their trajectory and targeting remain largely unperturbed in *sema-2b*$^{-/-}$ mutants. Axons of the "dorsomedial" classes Or22a and Or47a (C) normally choose ventromedial trajectories (arrowheads) to DM2 and DM3, respectively. In *sema-2b*$^{-/-}$ mutants, they aberrantly select dorsolateral trajectories (arrowheads), but target to the correct glomeruli. See Figure S1 for phenotypes of the 19 additional ORN classes analyzed.

(D) Schematic of the adult antennal lobe representing all 25 ORN classes examined in *sema-2b*$^{-/-}$ mutants, listed by target glomeruli and separated into three section planes along the anterior-posterior axis. Red, classes with both targeting and trajectory error; blue, unaffected classes; orange, classes with mostly trajectory errors; purple, CO_2-sensitive ORNs that target only ipsilateral V glomerulus.

(E) Quantification of phenotypes in *sema-2b*$^{-/-}$ mutant brains. Black, percentage of brains exhibiting mistargeted axons; gray, percentage of antennal lobe hemispheres exhibiting ectopic axon trajectories. Neither of these phenotypes was observed in wild-type controls. Number of mutant brains analyzed for each Or class is listed above each column pair. Compare with eyFlp MARCM phenotypes in Figure S2. Also see Figure S3 for analysis of mistargeting specificity.

Mistargeted ORN Axons Retain Target Specificity when Sema-2b Is Perturbed

Despite the widespread glomerulus distortion or displacement of *sema-2b*$^{-/-}$ brains, we observed that mistargeted axons from ventromedial ORN classes projected to specific regions of the antennal lobe rather than random locations. Indeed, in eyFlp MARCM, wayward *sema-2b*$^{-/-}$ axons of each ORN class targeted to specific sets of glomeruli that remained identifiable

(Figure S3A). These data suggest that axons that choose incorrect trajectories can still select preferred targets, perhaps by responding to local cues in other regions of the antennal lobe. We further tested mistargeting specificity by colabeling Or67b ORNs with one of three other ORN classes in *sema-2b* mutants (Figure S3B). In most cases, colabeled Or92a axons in the mutant brain mistargeted medially but nonadjacently to the ectopic Or67b target site (16/20 = 80% hemispheres), while Or98a axons mistargeted medially but adjacently (34/40 = 85% hemispheres, respectively) and Or35a axons mistargeted ventrally to ectopic Or67b axons (30/34 = 88% hemispheres). In all cases, ectopic axon termini from different ORN classes did not intermingle.

Since Sema-2b overexpression caused a significant decrease in the dorsolateral/ventromedial ratio (Figures 1F and 1H), we predicted that such overexpression would cause adult targeting defects in dorsolateral ORN classes. Indeed, a large fraction of Or67d and Or88a ORN axons mistargeted to the ventral antennal lobe when Sema-2b was overexpressed in all ORNs during development (Figure S3C). Furthermore, these mistargeted axons always projected to immediately adjacent regions much as in wild-type controls (18/18 hemispheres), with Or67d axons medial to Or88a axons in 89% of cases (16/18 hemispheres).

These observations suggest that mistargeted axons in Sema-2b loss- and gain-of-function contexts still exhibit targeting specificity and can retain relative interclass spatial relationships. They thus support a sequential model of ORN axon guidance in which Sema-2b primarily specifies the initial axon trajectory and thereby constrains target choice, while additional molecular cues subsequently govern targeting to specific glomeruli.

Loss of Plexin-B, the Sema-2b Receptor, Causes Nearly Identical Trajectory and Glomerular Choice Defects

We next explored the cellular mechanisms by which Sema-2b specifies ORN trajectory choice. Plexin B (PlexB) has been identified as a receptor for the secreted semaphorins Sema-2a and Sema-2b (Ayoob et al., 2006; Wu et al., 2011). Evidence from the embryonic ventral nerve cord supports a model in which Sema-2b acts as an attractive cue through PlexB to promote fasciculation of Sema-2b-expressing axons in specific longitudinal bundles (Wu et al., 2011). To test whether PlexB plays a role in ORN axon trajectory choice, we first examined ORN axon trajectories in *plexB*$^{-/-}$ mutants at 24 hr APF. Just as in *sema-2b*$^{-/-}$ mutants (Figure 1B), the dorsolateral axon trajectory was enlarged at the expense of the ventromedial trajectory (Figure 3A, compare middle and top rows; quantified in Figure 3B). Adult *plexB*$^{-/-}$ mutants also exhibited class-specific glomerular targeting defects nearly identical to those of *sema-2b* mutants (Figure 2): ventromedial ORN classes showed severe defects in both trajectory and target choice, dorsolateral classes were unaffected, and dorsomedial classes exhibited severe trajectory-choice defects but largely normal target selection (Figures 3C–3E; Figure S4). The striking similarities between *sema-2b*$^{-/-}$ and *plexB*$^{-/-}$ mutant phenotypes suggest that PlexB acts as a Sema-2b receptor in ORN axon trajectory choice, corroborating previous studies in the embryonic ventral nerve cord (Wu et al., 2011).

Plexin-B Also Acts in ORNs to Regulate ORN Trajectory Choice

We next asked which cells require PlexB for ORN trajectory choice. None of the anti-PlexB antibodies we produced allowed us to detect endogenous PlexB in the pupal brain. *plexB*'s location on the 4th chromosome also precludes MARCM-based mosaic analyses. We therefore tested cell-type-specific PlexB requirements using a transgenic rescue approach. Just as we determined for Sema-2b, PlexB expression in all ORNs using *pebbled-GAL4* was sufficient to rescue the ORN axon trajectory defects of *plexB*$^{-/-}$ mutants at 24 hr APF (Figure 3A, bottom; quantified in Figure 3D), indicating that PlexB acts ORN-autonomously to regulate axon trajectory choice. These data suggest that Sema-2b and PlexB mediate ORN axon-axon interactions to regulate trajectory choice.

Sema-2b Can Act Cell-Autonomously in ORNs to Specify Ventromedial Trajectory

How can a secreted protein such as Sema-2b act within ORNs to instruct ventromedial trajectory choice of individual axons? The fact that membrane-tethered Sema-2b can fully rescue the *sema-2b*$^{-/-}$ trajectory defects (Figure 1D) indicates that Sema-2b acts at short range. Below, we use two experiments to test whether Sema-2b can act cell-autonomously in ORNs to specify ventromedial trajectory.

First, we used hsFlp-based MARCM with late heat-shock time points to induce very small *sema-2b*$^{-/-}$ clones (Figure 4A). In all six ventromedial classes examined, labeled *sema-2b*$^{-/-}$ clones exhibited ectopic dorsolateral trajectories and severe mistargeting phenotypes just as with eyFlp MARCM clones or in whole-animal mutants (Figure 4B; Figure S5A; quantified in Figure 4C). This indicates that Sema-2b deletion in a small number of isolated ORNs is sufficient to cause both trajectory and glomerular targeting defects. Our use of specific hsFlp lines identified the class of labeled ORNs and aided phenotypic analysis. However, because each *Or-GAL4* only labeled a subset of hsFlp-induced mutant cells (Figure 3A), it remains possible that loss of Sema-2b in unlabeled "background" ORN clones contributed to the observed defects.

In a complementary experiment, we expressed Sema-2b™ in small *pebbled-GAL4*–labeled hsFlp MARCM clones in *sema-2b*$^{-/-}$ mutants. In this scenario, only labeled ORNs express Sema-2b (Figure 4D), allowing us to test whether isolated Sema-2b+ ORNs can rescue trajectory phenotypes in *sema-2b*$^{-/-}$ mutants. Fasciculation and filopodia extension of developing ORN axons hinders unequivocal axon counting within the antennal lobe. We therefore quantified the number of labeled ORNs by counting their somata within the antenna; by adjusting heat-shock timing and duration, we reduced the number of labeled ORNs to an average of ~10 isolated cells per antenna (Figures S5B and S5C), each of which contains a total of ~1,300 ORNs. In a control experiment where all cells were *sema-2b*$^{-/-}$, MARCM-labeled axons predominantly selected the dorsolateral trajectory (Figures 4E, top, and 4F), as expected from the developmental *sema-2b*$^{-/-}$ phenotype (Figure 1B). However, in experimental animals in which all cells were *sema-2b*$^{-/-}$ except a few MARCM-labeled ORNs expressing Sema-2b™, labeled axons took the ventromedial trajectory in the

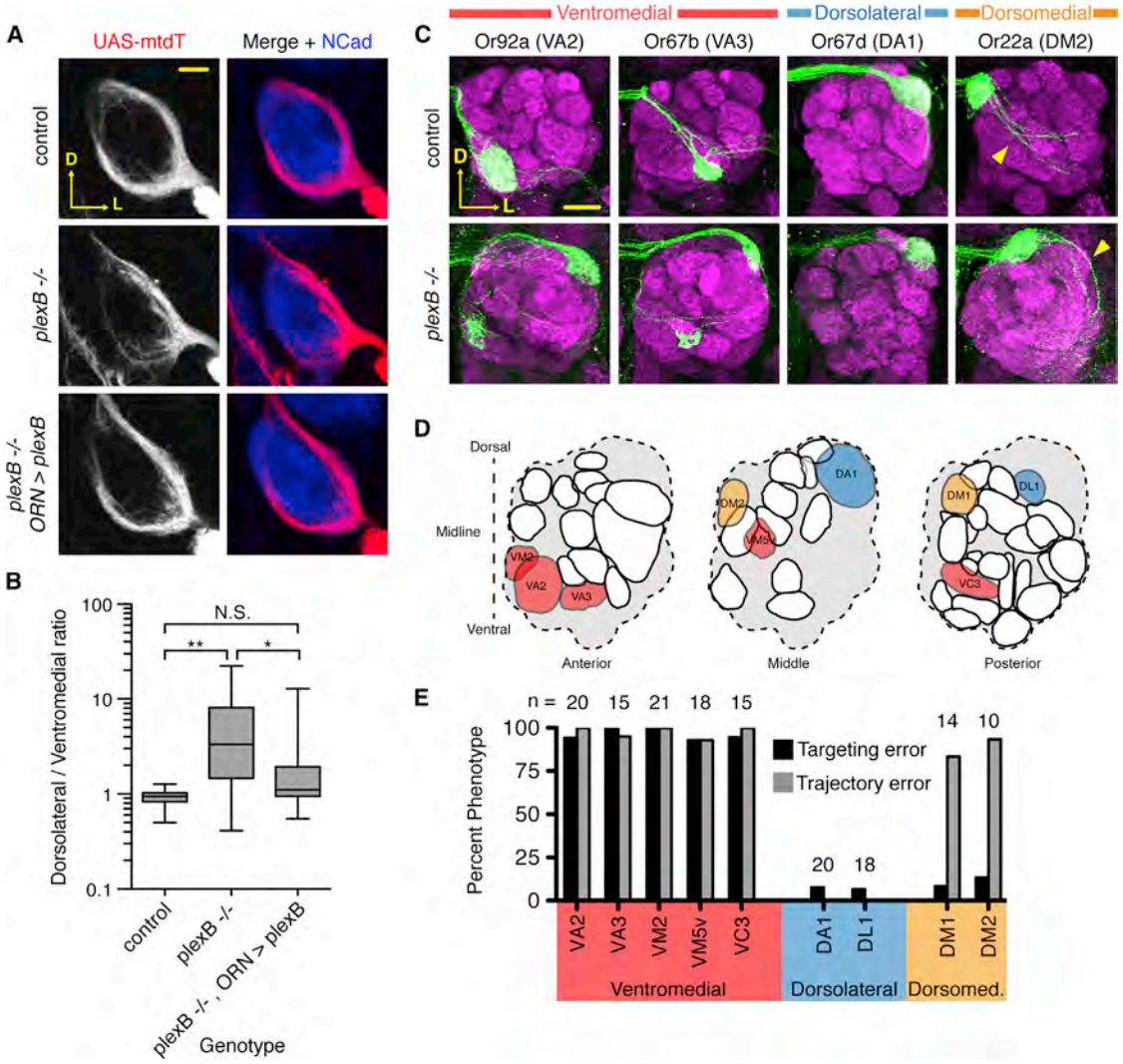

Figure 3. PlexB Acts in ORNs and Shares Nearly Identical Developmental and Adult Phenotypes with Sema-2b

(A) As in Figure 1A, developing ORN axons choose a ventromedial or dorsolateral trajectory at 24 hr APF in controls (top). In *plexB*$^{-/-}$ mutants, ORN axons primarily choose the dorsolateral trajectory, with a drastic reduction in the ventromedial axon bundle (middle). ORN-specific expression of *UAS-plexB* at 25°C rescues the ventromedial axon trajectory in *plexB*$^{-/-}$ mutants (bottom). All ORN axons are labeled by *pebbled-GAL4* driving *UAS-membrane-tagged tdTomato (mtdT)*, while N-Cadherin staining labels the antennal lobe neuropil.

(B) Quantification of dorsolateral/ventromedial axon bundle ratio, as in Figure 1H. Geometric means/sample sizes are as follows: control, 0.90/17; *plexB*$^{-/-}$, 3.45/19; *plexB*$^{-/-}$, *ORN* > *plexB*, 1.49/18. *p < 0.05; **p < 0.01; NS, not significant; one-way ANOVA with Bonferroni's multiple comparison test.

(C) Representative ventromedial, dorsolateral, and dorsomedial ORN classes labeled in control (top) or *plexB*$^{-/-}$ brains (bottom). As in *sema-2b*$^{-/-}$ brains, Or92a and Or67b axons exhibit trajectory and targeting phenotypes, while Or67d axons are largely unaffected, and Or22a axons primarily exhibit trajectory defects. See Figure S4 for phenotypes of additional classes.

(D and E) Schematic and quantification of trajectory and targeting defects for the 9 ORN classes examined in *plexB*$^{-/-}$ mutants, labeled as in Figure 2.

majority of cases (Figures 4E, bottom, and 4F). Remarkably, all of the nine examples of Sema-2b+ single-cell clones chose the ventromedial trajectory, while all three examples of single-cell clones in controls chose the dorsolateral trajectory.

Given that *pebbled-GAL4* labels all ORNs, a full rescue should restore a roughly 1:1 dorsolateral:ventromedial axon ratio (Figure 1C). The fact that all Sema-2b+ axons selected the ventromedial trajectory in nearly all experimental animals is more reminiscent of our overexpression experiments (Figures 1F and 1G). One possible explanation is a difference in overexpression levels: because the *UAS-sema-2b*^{TM} transgene is distal to the FRT site used for MARCM, two copies of *UAS-sema-2b*^{TM} transgenes were expressed in all MARCM clones. Since most unlabeled (and thus *sema-2b*$^{-/-}$) axons selected the dorsolateral trajectory, another possibility is that reduced competition for limiting central cues or physical space facilitates ventromedial trajectory choice in Sema-2b+ axons. Regardless of the specific mechanisms, sparsely restoring

Sema-2b expression in less than 1% of ORNs or even in single ORNs was sufficient for ventromedial targeting, demonstrating that Sema-2b can act cell-autonomously to instruct ventromedial axon trajectory choice (see Figure 7 and Discussion).

Sema-2b Also Acts Non-Cell-Autonomously in ORNs

While Sema-2b can act cell-autonomously to direct ventromedial ORN targeting, Sema-2b produced from ventromedial-targeted ORN axons may also serve as a ligand to attract other PlexB/Sema-2b+ ORN axons (Figure 3, and see Figure 7). To test potential non-cell-autonomous functions of Sema-2b, we performed eyFlp reverse MARCM (Komiyama et al., 2004), in which up to 50% of all ORNs are *sema-2b*$^{-/-}$ and only WT ORN axons are labeled (Figure 4G). If Sema-2b acts strictly cell-autonomously, WT ORN axons should target normally in these mosaic animals. However, we found significant targeting defects in multiple ventromedial ORN classes. This is consistent with the idea that Sema-2b from ORNs also acts as a ligand to mediate axon-axon interactions, thereby promoting ventromedial trajectory choice and targeting. Interestingly, we observed variable penetrance between different classes (Figures 4H and 4I; Figure S5D). Or49b and Or98a ORNs, targeting to VA5 and VM5v, respectively, were largely normal in eyFlp reverse MARCM (Figure 4I) but exhibited the most penetrant phenotypes in hsFlp MARCM (Figure 4C). The simplest interpretation is that axons from Or49b and Or98a ORNs arrive at the antennal lobe earlier than axons of other classes and therefore rely primarily on cell-autonomous Sema-2b function to detect central cues (see next section).

Sema-2a and Sema-2b from the Central Brain Orient ORN Axon Trajectory Choice

While Sema-2b/PlexB-mediated attractive ORN axon-axon interactions can account for why Sema-2b+ axons select a common trajectory, they cannot explain why Sema-2b+ axons *always* choose the ventromedial trajectory. A possible scenario would be for an external cue to bias the initial choice and orient it with respect to the antennal lobe, after which Sema-2b/PlexB-mediated axon-axon interactions can further consolidate Sema-2b+ axons into a common trajectory.

We have previously shown that Sema-2a and Sema-2b act redundantly to regulate PN dendrite targeting before the arrival of pioneering adult ORN axons. Specifically, Sema-2a and Sema-2b derived from degenerating larval ORNs and developing adult PNs form a ventromedial-high/dorsolateral-low concentration gradient, thereby directing Sema-1a-dependent PN dendrite targeting along this axis (Sweeney et al., 2011). Indeed, both Sema-2a and Sema-2b were still enriched ventromedially within the antennal lobe at 24 hr APF (Figure 1A$_2$; Figure S6A) and could thus act as orienting cues for incoming adult axons. To test this idea, we first examined ORN axon trajectory choice in *sema-2a*$^{-/-}$, *sema-2b*$^{-/-}$ double mutants. We found similar axon trajectory choice defects (Figure 5A; quantified in Figure 5B) as in *sema-2b* mutants (Figures 1B and 1H) or *plexB* mutants (Figures 3A and 3B). These data indicate that in the absence of Sema-2a/2b/PlexB signaling, most ORN axons take the dorsolateral trajectory by default.

Next, we used *pebbled-GAL4* to express Sema-2b in ORNs of *sema-2a*$^{-/-}$, *sema-2b*$^{-/-}$ double mutants, to specifically test the role of central Sema-2a/2b while keeping Sema-2b/PlexB-mediated ORN axon-axon interactions intact. To restrict Sema-2b expression to adult ORNs only, we also included *Orco-GAL80*, which can suppress *pebbled-GAL4* in larval ORNs throughout their development (Figures S6F and S6G). We found that the trajectory of Sema-2b-expressing ORNs fell into three groups under these conditions. In 15% of cases (n = 4/27), axons were split between the dorsolateral and ventromedial trajectories (Figure 5C, top). In the remaining 85% of cases, however, all axons exclusively chose either the ventromedial (12/27) or dorsolateral (11/27) trajectory, with nearly equal probability (Figure 5C, middle and bottom). These results indicate that centrally derived Sema-2a and Sema-2b are essential to bias ORN axon trajectory choice. *sema-2a*$^{-/-}$ single mutants did not exhibit significant ORN mistargeting phenotypes, and Sema-2b overexpression was sufficient to bias axons to the ventromedial trajectory even in *sema-2a* mutants (Figures S6B–S6E). Thus, central Sema-2a and Sema-2b act similarly and redundantly in orienting incoming ORN axons. In the absence of these central cues, ORN axons were equally likely to choose ventromedial or dorsolateral trajectories. The fact that all Sema-2b+ axons bundle together in 85% of cases supports the idea that Sema-2b/PlexB-mediated axon-axon signaling—which remained intact in this experiment—was sufficient to consolidate axons into single bundles, even though trajectory choice became stochastic.

Sema-2b Expression Is Negatively Regulated by Notch Signaling in ORNs

What mechanisms regulate Sema-2b expression and restrict it to ventromedial ORNs? A previous study demonstrated that the Notch pathway diversifies ORN identities and organizes their axonal projections (Endo et al., 2007). Specifically, asymmetric Notch-pathway activation divides ORNs within each sensillum into Notch-ON and Notch-OFF classes with distinct axonal trajectories and targeting decisions. In the majority of cases, Notch-ON and Notch-OFF ORNs from the antenna respectively select dorsolateral and ventromedial axon trajectories. These observations led us to hypothesize that (1) the Notch pathway regulates Sema-2b expression, and (2) Sema-2b acts downstream of Notch to specify axon trajectory choice.

To test these hypotheses, we utilized *AM29-GAL4*, which labels the two ORN classes that reside within the ab10 sensillum: the Notch-ON ORN takes a dorsolateral trajectory and projects to the DL4 glomerulus, while the Notch-OFF ORN takes a ventromedial trajectory and projects to DM6 (Endo et al., 2007). To test whether the Notch pathway regulates Sema-2b expression, we first used *AM29-GAL4*-based MARCM labeling to specifically visualize pairs of ORNs within the ab10 sensillum. We found that Sema-2b protein was enriched as perinuclear particles in only one cell of each AM29$^+$ ORN pair at 36 hr APF (Figure 6A$_1$). These perinuclear particles likely correspond to Sema-2b protein in the secretory pathway, as they were absent from both cells in *sema-2b*$^{-/-}$ paired MARCM clones (Figure 6B$_1$). To examine whether the Notch pathway regulates Sema-2b distribution, we used MARCM to generate AM29$^+$ paired clones mutant for *mastermind* (*mam*), a core component of the Notch-activated

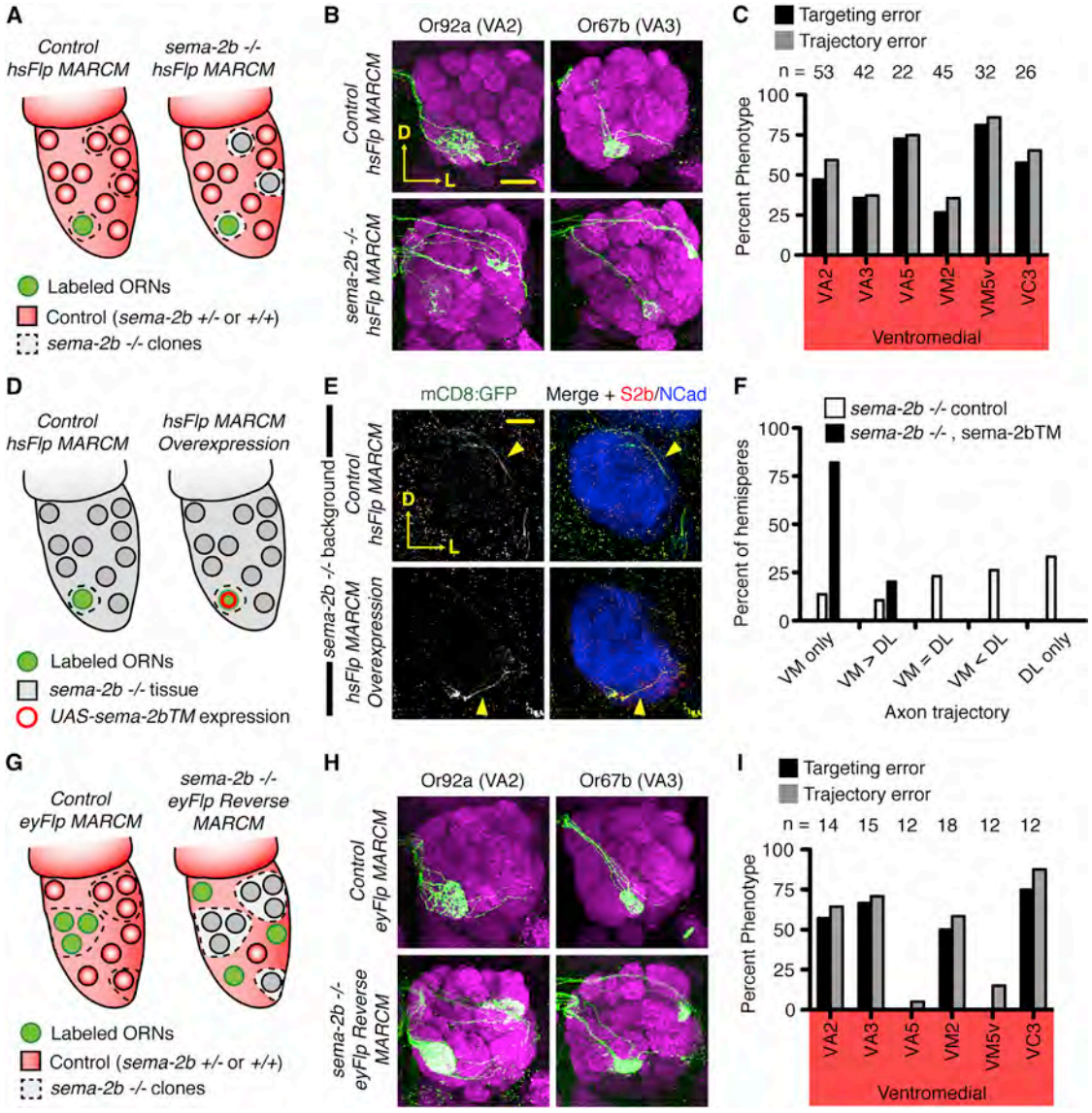

Figure 4. Cell-Autonomous and Nonautonomous Sema-2b Functions

(A) Schematic of loss-of-function hsFlp MARCM. (Left) hsFlp MARCM generates small and sparse ORN clones (dotted lines; compare with eyFlp MARCM in Figure S2), a subset of which is labeled with class-specific *Or-GAL4* lines. In control MARCM, all cells, and thus all clones, are WT; (Right) In *sema-2b*$^{-/-}$ hsFlp MARCM, all labeled cells are *sema-2b*$^{-/-}$, but only a subset of *sema-2b*$^{-/-}$ ORNs expressing a given *Or-GAL4* is labeled. Green, *Or-GAL4*-labeled ORNs; gray, *sema-2b*$^{-/-}$ clones; red, control (*sema-2b*$^{+/-}$ or *sema-2b*$^{+/+}$).

(B) Control (top) and *sema-2b*$^{-/-}$ (bottom) hsFlp MARCM small clones of mCD8:GFP-labeled axons (green). Or92a and Or67b *Sema-2b*$^{-/-}$ axons aberrantly choose dorsolateral trajectories and mistarget dorsolaterally within the antennal lobe. As with whole-animal mutants or eyFlp MARCM, some axons can remain unaffected and target properly. Animals between 0 and 24 hr APF were heat shocked for 10 min at 37°C to induce clones.

(C) Quantification of hsFlp MARCM trajectory and targeting phenotypes, labeled analogously to previous figures. Different classes exhibit varying penetrance; Or49b (VA5) and Or98a (VM5v) axons are the most severely affected.

(D) Schematic of the *pebbled-GAL4*-based MARCM overexpression approach. (Left) As before, hsFlp MARCM generates small and sparse ORN clones in a *sema-2b*$^{-/-}$ background. Thus, all cells are mutant and a small number of ORNs are labeled with mCD8:GFP. (Right) In experimental animals, labeled ORNs are the only cells in the antennae that express *UAS-sema-2b*^{TM}. Grey, *sema-2b*$^{-/-}$ tissue; green, *pebbled-GAL4*-labeled ORNs; red, Sema-2b™-expressing ORNs.

(E) Representative 24-hr-APF antennal lobes from *sema-2b*$^{-/-}$ animals with control (top) or Sema-2b™-overexpressing (bottom) ORNs. 0-hr-APF animals were heat shocked for 5–10 min at 37°C to induce clones. (Left) ORN axons labeled with mCD8:GFP. (Right) Overlay of left panel with Sema-2b (red) and NCad (blue) staining. Arrowheads, labeled axons.

(F) Quantification of axon-trajectory phenotypes in *pebbled-GAL4* hsFlp MARCM. See Experimental Procedures for details. n (antennal lobe hemispheres) = 32 *sema-2b*$^{-/-}$ controls, and 41 *sema-2b*$^{-/-}$, *UAS-sema-2b*^{TM} mutants.

(G) Schematic of the reverse eyFlp MARCM approach. (Left) WT control eyFlp MARCM as in Figure S2. (Right) In *sema-2b*$^{-/-}$ eyFlp reverse MARCM, up to 50% of ORNs are homozygous mutant for *sema-2b*, but only WT ORNs are labeled by class-specific *Or-GAL4* lines. Green, *Or-GAL4*-labeled ORNs; gray, *sema-2b*$^{-/-}$ clones; red, control (*sema-2b*$^{+/-}$ or *sema-2b*$^{+/+}$).

(legend continued on next page)

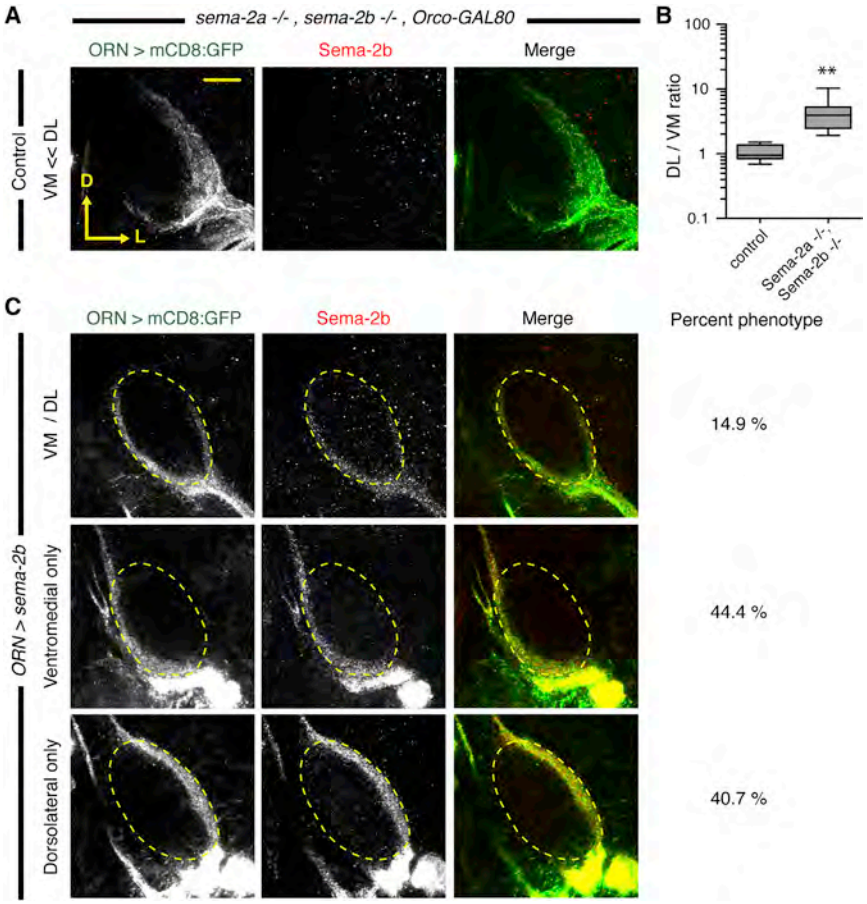

Figure 5. Central Sema-2a and Sema-2b Bias Initial Axon Trajectory Choice

(A) *sema-2a*$^{-/-}$, *sema-2b*$^{-/-}$ double-mutant brains at 24 hr APF, in which *pebbled-GAL4* drives mCD8:GFP in all adult ORNs. Axons predominantly choose dorsolateral trajectories, just as in *sema-2b* or *plexB* mutants.

(B) Quantification of dorsolateral/ventromedial axon bundle ratio, as in Figure 1H. Control = 1.02, n = 6; *sema-2a*$^{-/-}$, *sema-2b*$^{-/-}$ = 3.91, n = 11; **p < 0.01; unpaired t test.

(C) *sema-2a*$^{-/-}$, *sema-2b*$^{-/-}$ double-mutant brains at 24 hr APF, in which *pebbled-GAL4* drives mCD8:GFP as well as Sema-2b expression in all adult ORNs, but not in larval ORNs due to the presence of *Orco-GAL80* (see Figure S6). Images show all ORN axons labeled by *UAS-mCD8:GFP* (left), Sema-2b staining (middle), and an overlay of the left and middle panels (right). (Top row) Representative image in which ORNs choose both ventromedial and dorsolateral trajectories (4/27 = 14.9% hemispheres). (Middle row) Representative image in which all ORN axons choose the ventromedial trajectory (12/27 = 44.4% hemispheres). (Bottom row) Representative image of an antennal lobe in which all ORN axons choose the dorsolateral trajectory (11/27 = 40.7% hemispheres).

See Figure S6 for Sema-2a expression patterns and loss-of-function phenotypes.

transcriptional complex (Kovall, 2008). Strikingly, Sema-2b was present in both cells of *mam*$^{-/-}$ paired clones (Figure 7C$_1$), indicating that Notch signaling normally represses Sema-2b in one cell of each AM29^{+} pair (Figures 6A$_3$–6C$_3$).

Sema-2b Mediates Notch-Pathway Output for ORN Trajectory Choice

To examine the functional consequences of Notch-mediated Sema-2b repression in ORN axon targeting, we analyzed axon trajectory and glomerular targeting for *AM29*$^{+}$ paired MARCM clones. In WT paired clones, one ORN took the ventromedial trajectory to DM6, whereas its partner took a dorsolateral trajectory to DL4 (Figures 6A$_2$ and 6A$_3$, 16/16 clones). In *mam*$^{-/-}$ paired clones, both axons adopted a ventromedial trajectory and targeted to DM6 (Figures 6C$_2$ and 6C$_3$, 22/22 clones), in accordance with previous results (Endo et al., 2007). In *sema-2b*$^{-/-}$ paired clones, however, both axons projected dorsolaterally to their targets in most cases (Figures 6B$_2$ and 6B$_3$; 17/22 = 77.3% clones), confirming that Sema-2b is essential for ventromedial axon pathway choice. Because *sema-2b* and *mam* reside on the same chromosome arm, we used MARCM to test double mutants. Remarkably, in *sema-2b*$^{-/-}$, *mam*$^{-/-}$ double-mutant paired clones, both neurons chose a dorsolateral axon trajectory, a phenotype opposite to that of *mam*$^{-/-}$ paired clones (Figure 6D$_2$ and 6D$_3$; 32/37 clones; Figure 6E, compare rightmost two columns). Together with the fact that *mam* negatively regulates Sema-2b expression, this epistasis experiment demonstrates that *sema-2b* acts downstream of *mam*. Furthermore, since additional loss of *sema-2b* reverted *mam*$^{-/-}$ axon trajectory choice phenotypes, these results also indicate that Sema-2b alone accounts for Notch-pathway-mediated axon trajectory choice.

Interestingly, Sema-2b removal only partially reverted the *mam*$^{-/-}$ phenotype in glomerular targeting, as double-mutant axons skipped the DL4 glomerulus in 46% of clones despite taking the correct dorsolateral trajectory that passed by the target DL4 glomerulus (17/37 clones; Figure 6D$_2$, compare top and bottom; quantified in Figure 6F). Notch signaling thus regulates other factors in addition to Sema-2b to direct glomerular target choice.

(H) Control eyFlp MARCM (top) and *sema-2b*$^{-/-}$ eyFlp reverse MARCM (bottom) clones of mCD8:GFP-labeled axons (green). In the presence of background *sema-2b*$^{-/-}$ clones, WT Or92a and Or67b axons exhibit trajectory and targeting phenotypes similar to those of mutant axons.

(I) Quantification of eyFlp reverse MARCM phenotypes. Most classes exhibited trajectory and targeting phenotypes comparable to those of hsFlp MARCM, with the exception of Or49b and Or98a ORNs, which remained largely normal. Notably, these two classes were the most severely affected in hsFlp MARCM (C). See Figure S5 for MARCM analyses of additional ORN classes and cell-body counts for MARCM rescue.

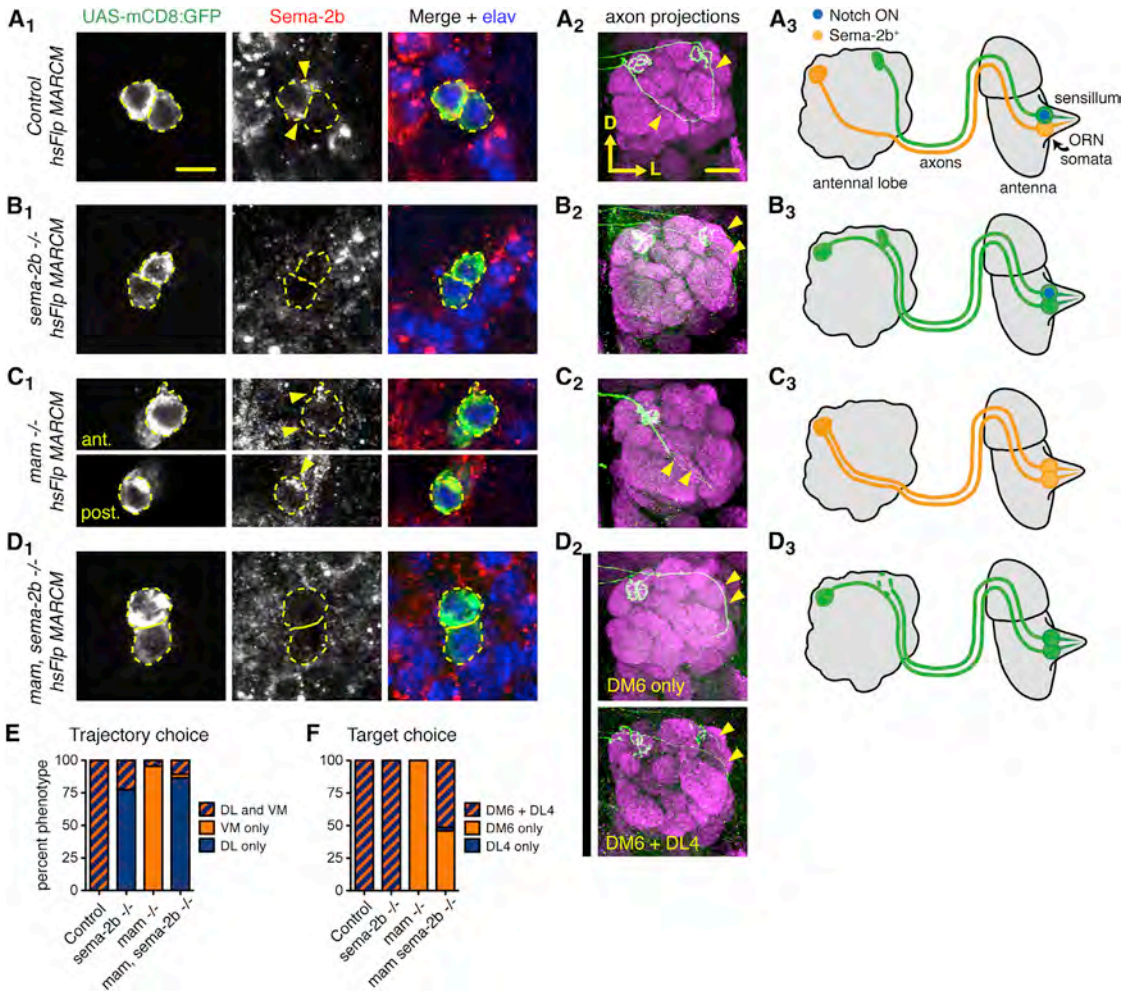

Figure 6. Sema-2b Is Repressed by the Notch Pathway and Mediates Trajectory Choice Downstream of the Notch Pathway

(A_1–A_3) (A_1, left) Wild-type AM29+ paired clones generated by hsFlp MARCM and labeled with mCD8:GFP, (A_1, middle) Sema-2b protein is selectively enriched in one cell of each paired clone (12/12 clones). Arrowheads point to Sema-2b puncta. (A_1, right) Overlay of left and middle panels. Elav immunostaining labels neuronal nuclei; ORN cell bodies are outlined in yellow. Scale bar = 5 μm. (A_2) Axonal projections from wild-type AM29+ paired clones. One cell takes a ventromedial trajectory and selects the DM6 glomerulus, while the other takes a dorsolateral trajectory and selects the DL4 glomerulus (16/16 clones). Yellow arrowheads mark axon trajectories. (A_3) Summary schematic of Sema-2b expression and axonal projection patterns for wild-type paired clones. Green, MARCM-labeled AM29+ paired clones; yellow, Sema-2b enrichment; blue, activated Notch signaling according to Endo et al. (2007).

(B_1–B_3) (B_1) Immunostaining confirms absence of Sema-2b signal in *sema-2b*$^{-/-}$ paired clones. (B_2) Both axons from *sema-2b*$^{-/-}$ mutant clones take dorsolateral trajectories (17/22 = 77.3% clones), but target correctly to DM6 and DL4 (22/22 clones). (B_3) Summary schematic.

(C_1–C_3) (C_1) Sema-2b is expressed in both cells of *mam*$^{-/-}$ paired clones (arrowheads, 15/15 clones); images show the anterior section (top row) and posterior section (bottom row) of the same paired clone. (C_2) Both axons of *mam*$^{-/-}$ paired clones take ventromedial trajectories and select the DM6 glomerulus (22/22 clones). (C_3) Summary schematic; removing *mam* derepresses Sema-2b expression and thus causes axons to choose ventromedial trajectories.

(D_1–D_3) (D_1) As expected, Sema-2b is absent in *mam*$^{-/-}$, *sema-2b*$^{-/-}$ double-mutant clones. (D_2) Both axons from double-mutant clones take dorsolateral trajectories (32/37 = 86.5% clones); shown at top is an example in which axons do not innervate the DL4 glomerulus (17/37 = 46% clones) and at bottom an example with normal targeting to DM6 and DL4 (20/37 = 54% clones). (D_3) Summary schematic; Sema-2b removal reverts the *mam*$^{-/-}$ phenotype with respect to trajectory choice, but only partially "rescues" target selection as represented by the dashed DL4 glomerulus.

(E) Quantification of trajectory-choice phenotypes. Orange/blue hatched, one dorsolateral trajectory and one ventromedial trajectory; orange, ventromedial trajectory only; blue, dorsolateral trajectory only.

(F) Quantification of target-selection phenotypes. Orange/blue hatched, one DL4 terminus and one DM6 terminus; orange, DM6 only; blue, DL4 only.

See Figure S7 for epistatic analyses of additional ORN classes.

To test how generally Notch regulates Sema-2b, we extended our phenotypic and epistasis analyses to the ab1 and at2 sensilla. In each case, we used two Or-GAL4 lines to label a dorsolateral (Notch ON) and a ventromedial (Notch OFF) ORN class each, and used hsFLP MARCM to manipulate the genotype of labeled ORNs. Just as in AM29^{+} paired clones, we found that Sema-2b was required for ventromedial trajectory and was epistatic to *mam* (Figure S7). Thus, Sema-2b mediates axon

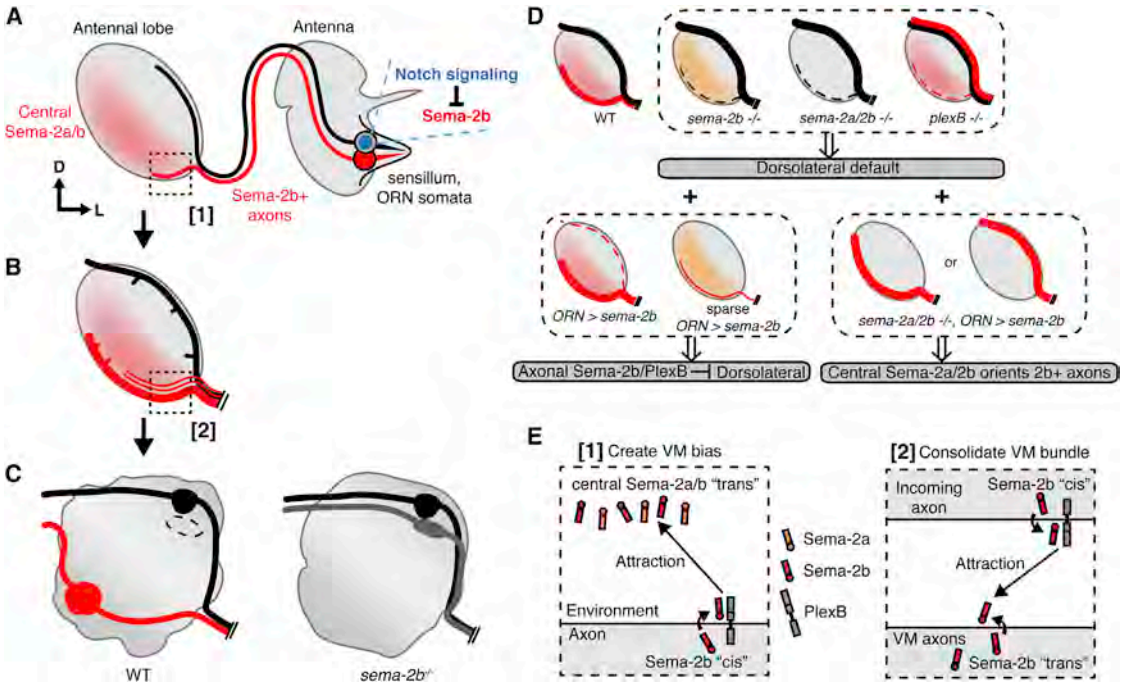

Figure 7. Summary of Sema-2b Function in ORN Axon Trajectory

(A) Sema-2b is expressed only in ventromedial ORN classes (right, red cell) due to its repression by Notch signaling in dorsolateral classes (right, blue cell). Sema-2a and Sema-2b from projection neurons and degenerating larval ORN axons (left, Central Sema-2a/2b, red shading) regulate PN dendrite patterning earlier in development (Sweeney et al., 2011) but remain ventromedially enriched within the antennal lobe and function as orientation cues for incoming Sema-2b+ axons (red), biasing them ventromedially. Expansion of dashed box 1 is shown at left in (E). D, dorsal; L, lateral.

(B) Sema-2b and its receptor PlexB mediate axon-axon interactions to reinforce the ventromedial bias generated in (A) and promote ventromedial axon bundle formation. Expansion of dashed box 2 is shown at right in (E).

(C) Proper developmental trajectory choice is essential for final target selection in ventromedial (red) ORN classes. In WT (left), the ventromedial trajectory of Sema-2b+ axons constrains them against selecting possible targets in the dorsolateral region of the antennal lobe (dotted outline). In *sema-2b* mutants (right), ventromedial ORNs choose dorsolateral trajectories that prevent them from reaching proper targets. Instead, they mistarget to specific dorsolateral target areas, likely in response to cell-surface cues that remain intact. The dorsolateral class (black) is unaffected in *sema-2b* mutants.

(D) Summary of key experiments and phenotypes for axon trajectory choice at 24 hr APF. (Top left) In WT, Sema-2b+ axons (red) choose the ventromedial trajectory, while Sema-2b– axons (black) choose the dorsolateral trajectory. (Top right) In *sema-2b*, *sema-2a/2b*, or *plexB* mutants, axons predominantly select the dorsolateral trajectory, indicating a "dorsolateral default" in the absence of Sema-2b/PlexB signaling. Orange shading in the *sema-2b* antennal lobe depicts remaining Sema-2a. (Bottom left) Pan-ORN Sema-2b overexpression in WT brains causes most ORNs to select the ventromedial trajectory. Similarly, sparse or single MARCM-based Sema-2b overexpression in a *sema-2b*$^{-/-}$ background causes labeled axons to select the ventromedial trajectory. Orange shading depicts remaining central Sema-2a. Together with the mutant analyses above and ORN-specific PlexB rescue (Figure 3A), these data suggest that Sema-2b/PlexB signaling suppresses the dorsolateral default. (Bottom right) The stochastic trajectory choice of entire bundles in the absence of central Sema-2a/2b demonstrates the importance of these target zone-derived cues in orienting incoming Sema-2b+ axons. Intact axonal Sema-2b/PlexB signaling consolidates all axons into single bundles.

(E) A speculative model of cellular mechanisms of Sema-2b function. (Left) For pioneering axons, Sema-2b expressed in *cis* may form a complex with PlexB, sensitizing it to the attraction of centrally derived Sema-2a and Sema-2b in *trans* (arrow), creating a ventromedial trajectory bias (Figure 7A, dashed box 1). (Right) For late-arriving axons, *cis* Sema-2b may likewise sensitize PlexB to *trans* Sema-2b from preceding ventromedial (VM) axons. Sema-2b/PlexB thus mediate attractive axon-axon interactions that consolidate initial trajectory choice (Figure 7A, dashed box 2).

trajectory choice downstream of Notch signaling in multiple ORN classes.

DISCUSSION

Our analyses of Sema-2b function have revealed multiple cellular and molecular mechanisms that contribute to ORN targeting specificity. Chronologically, Notch signaling first limits Sema-2b expression to ventromedial ORNs (Figure 7A, right). Secreted Sema-2a and Sema-2b from the central brain then bias the trajectory choice of these Sema-2b+ ORN axons once they reach the antennal lobe (Figure 7A, left), after which Sema-2b/PlexB-mediated ORN axon-axon interactions consolidate this trajectory choice and promote ventromedial bundle formation (Figure 7B). Ultimately, choosing an appropriate developmental trajectory is crucial for proper target selection in ventromedial ORN classes (Figure 7C).

From ORN Fate to Trajectory Choice: The Notch Pathway Specifies Differential Sema-2b Expression

The Notch pathway regulates numerous developmental events in both invertebrates and vertebrates, and its classic roles in

specifying cell fate in the peripheral and central nervous systems is well established (Louvi and Artavanis-Tsakonas, 2006). The diversification of cell fates within individual sensilla (Endo et al., 2007) is an excellent example of how Notch determines neuronal fate, with specific consequences for axon targeting. While Notch has been proposed to act through a transcription-independent cytosolic pathway to regulate axon patterning (Kuzina et al., 2011), ORN axon targeting appears to utilize canonical transcriptional regulation, given its dependence on the transcriptional coactivator Mastermind (Endo et al., 2007). Canonical Notch activity has been shown to regulate axon and dendrite development in multiple contexts in vertebrates and invertebrates (e.g.: Sestan et al., 1999; Redmond et al., 2000; Langen et al., 2013; Li et al., 2013).

Here, we identified Sema-2b as a crucial downstream target in Notch-mediated ORN axon targeting (Figure 7A). Sema-2b expression is negatively regulated by Notch signaling, thus establishing a molecular difference between Notch-ON and Notch-OFF ORNs. Moreover, *sema-2b* and *mam* mutant ORNs exhibit opposite trajectory choice defects, while *sema-2b, mam* double-mutant ORNs phenocopy *sema-2b* mutant ORNs. These data cumulatively indicate that Sema-2b acts downstream of the Notch pathway and that Sema-2b is the primary mediator of Notch-pathway effects on ORN trajectory choice.

However, Sema-2b is unlikely to account for all aspects of Notch-mediated ORN fate diversification, as our double-mutant analysis indicates that synaptic target choice relies on additional Notch targets independent of Sema-2b (Figures 6D$_2$–6F). The specific mechanism by which Notch signaling represses Sema-2b expression in select ORNs is currently unknown. Notch may directly repress Sema-2b transcription or indirectly reduce Sema-2b mRNA or protein stability posttranscriptionally. Indeed, our observation that Sema-2b protein levels were significantly lower in dorsolateral ORN (Notch ON) axons compared to ventromedial (Notch OFF) axons despite pan-ORN GAL4-driven expression (Figure 1H, inset) favors an indirect posttranscriptional regulation of Sema-2b by the Notch pathway. While these possibilities remain to be investigated in future studies, our identification of an axon guidance molecule downstream of Notch provides an instructive example of how a fate decision is translated into an axon guidance decision.

Sema-2b Acts across Multiple Steps to Instruct Axon Trajectory Choice

Our genetic analyses have uncovered multiple mechanisms that ensure proper axon trajectory choice when ORN axons first arrive at the antennal lobe (Figure 7D). Below, we first summarize these findings based on our genetic data and then place these findings in developmental and cell biological context.

In WT (Figure 7D, top left), Sema-2b+ axons (red) choose the ventromedial trajectory and Sema-2b– axons (black) choose the dorsolateral trajectory. However, most axons in *sema-2b* mutants, *plexB* mutants, or *sema-2a sema-2b* double mutants choose the dorsolateral trajectory (Figure 7D, top right). This indicates that the dorsolateral trajectory becomes the default in the absence of Sema-2b/PlexB signaling. Since overexpressing Sema-2b in all ORNs causes most axons to take ventromedial trajectories, while sparse overexpression in isolated ORNs in *sema-2b* mutants (Figure 7D, bottom left) or PlexB expression in all ORNs in *plexB* mutants (not shown in Figure 7) can restore the ventromedial trajectory, we deduce that axonal Sema-2b and PlexB signaling vetoes the dorsolateral default pathway. Finally, since removing central Sema-2a/2b while maintaining Sema-2b/PlexB signaling in ORNs results in stochastic trajectory choice of the entire axon bundle (Figure 7D, bottom right), we infer that axonal Sema-2b/PlexB is sufficient to cause all Sema-2b+ axons to take the same trajectory, while central Sema-2a/2b is normally required to bias the trajectory choice of Sema-2b+ axons ventromedially.

Axon-axon interactions are widely used to establish wiring specificity in complex circuits of vertebrates and invertebrates (Sanes and Yamagata, 2009). In the fly olfactory system, for example, Sema-1a produced by early-arriving antennal ORN axons acts as a repulsive cue to constrain glomerular target selection of late-arriving maxillary palp ORN axons (Sweeney et al., 2007). Here, we show that Sema-2b/PlexB-mediated ORN axon-axon interactions regulate the trajectory choice of individual ORN axons when they first arrive at the antennal lobe, well before their final glomerular target selection. This mechanism is thus reminiscent of pretarget axon sorting as described for mammalian ORN axon targeting along the anterior-posterior axis of the olfactory bulb (Imai et al., 2009).

However, axon-axon interactions alone are insufficient to produce highly stereotyped neural maps and likely require external cues for proper orientation. We have identified central Sema-2a and Sema-2b as important orienting cues. In their absence, most Sema-2b+ ORNs can still form bundles, presumably through Sema-2b/PlexB-mediated axon-axon interactions, but their trajectory choice becomes stochastic (Figure 5). This experiment thus illustrates how target-derived and axon-derived cues cooperate to specify ORN trajectory choice: central Sema-2a/2b bias Sema-2b+ axons toward ventromedial trajectories (Figure 7A, left); ORN axon-derived Sema-2b subsequently acts as a cue to attract more Sema-2b+ axons to the same trajectory through the PlexB receptor (Figure 7B). Indeed, our mosaic analyses support both cell-autonomous and nonautonomous roles for Sema-2b in ORN axon targeting (Figure 4).

In summary, Sema-2b mediates multiple complementary processes during ORN and PN development. (1) Between 0 and 18 hr APF, larval ORN- and PN-derived Sema-2b, along with Sema-2a, form a ventromedial > dorsolateral concentration gradient in the developing antennal lobe to instruct PN dendrite targeting along this axis (Sweeney et al., 2011). (2) The Sema-2a/2b gradient persists through 24 hr APF to bias the trajectory choice of pioneering Sema-2b+ ventromedial ORN axons. (3) Sema-2b on ORN axons acts as a ligand to mediate bundle formation and consolidate trajectory choice. (4) Sema-2b in ORN axons also acts cell-autonomously in steps 2 and 3 to guide Sema-2b+ axons to take the ventromedial trajectory (Figures 7A and 7B). Thus, Sema-2b acts four times in consecutive stages of olfactory circuit wiring and serves as a molecular link between PN dendrite targeting and ORN axon targeting well before final synaptic matching.

A Possible Mechanism of Sema-2b Function: Cell-Autonomously Sensitizing PlexB to External Semaphorins

While secreted semaphorins are classic extracellular ligands for axon guidance (Kolodkin and Tessier-Lavigne, 2011), our mosaic genetic analyses demonstrate surprisingly that Sema-2b can act cell-autonomously to instruct ORN axon trajectory choice. In this context, Notch regulation of Sema-2b in individual ORNs ensures differential expression of this instructive molecule in different ORN classes.

How can a secreted molecule act cell-autonomously to instruct a guidance choice? Given the nearly identical phenotypes of *plexB* and *sema-2b* mutants (this study) and high-affinity binding of Sema-2b to PlexB-expressing neurons (Wu et al., 2011), we propose that Sema-2b cell-autonomously primes or sensitizes PlexB in such a way that it acts as an attractive receptor for external Sema-2a and Sema-2b. In one potential scenario, Sema-2b and PlexB expressed in *cis* (within the same cell) may form a complex that signals attraction in response to external Sema-2a/2b in *trans* (Figure 7E). This model explains both how centrally derived Sema-2a/2b orients pioneering Sema-2b+ ORN axons (Figure 7A, dashed box 1, and 7E, left) and how "follower" axons utilize ORN-derived Sema-2b for axon-axon interactions and bundle formation (Figures 7A, dashed box 2, and 7E, right). This proposal most parsimoniously explains our genetic and mosaic analyses and is fully consistent with Sema-2b+ axon tract formation in the embryonic ventral nerve cord (Wu et al., 2011). However, it awaits future biochemical studies for further validation.

cis interactions between an axon guidance molecule and a receptor have previously been documented for vertebrate Ephrin/Eph receptor signaling (Hornberger et al., 1999; Marquardt et al., 2005; Carvalho et al., 2006; Kao and Kania, 2011) and for a vertebrate class-6 transmembrane semaphorin (Haklai-Topper et al., 2010). While these studies suggest *cis* attenuation of receptor activity by a membrane-tethered ligand (Yaron and Sprinzak, 2012), our data support the notion that secreted ligands can participate in *cis* interactions to promote or sensitize guidance-receptor signaling, thus expanding the function of ligand-receptor *cis* interactions in axon guidance.

Trajectory Choice Constrains Glomerular Target Choice

Neural circuit wiring is a complex task: in the *Drosophila* olfactory circuit, each ORN must reach the antennal lobe and choose 1 of 50 possible postsynaptic targets with high precision. One strategy to reduce this complexity is to create hierarchical steps, such that axons face fewer simultaneous choices per step. Our genetic analysis of Sema-2b function in ORN axon targeting demonstrates this principle. ORN axons must make a binary decision soon after arriving at the antennal lobe: individual axons take either the ventromedial or dorsolateral trajectory, based on whether they express Sema-2b or not. Proper trajectory is crucial to place ventromedial ORNs in the correct target region for subsequent partner matching and synapse formation. Ventromedial ORNs that select incorrect trajectories early on cannot recover and ultimately make ectopic target choices (Figures 2 and 7C).

Interestingly, mistargeted axons in either Sema-2b loss- or gain-of-function conditions retain specificity in target choice (Figure S3), indicating that at least a subset of targeting cues remains functional in both cases. This observation also suggests that cell-surface molecules that mediate synaptic partner matching may be distributed throughout the antennal lobe for reiterative use instead of being restricted to select regions. Indeed, Teneurin-m instructs synaptic partner matching in dorsolateral glomeruli but is also expressed throughout the antennal lobe in a "salt and pepper" fashion (Hong et al., 2012); ORNs with aberrant trajectories may utilize cues such as Teneurin-m to select specific partners, albeit in incorrect target regions. Early developmental trajectory choice thus plays an important role in disambiguating cell-surface cues presented by different parts of the antennal lobe. Ultimately, our analysis of Sema-2b illustrates how a relatively small number of molecules can establish complex neural architecture with the help of sophisticated spatial and temporal regulation.

EXPERIMENTAL PROCEDURES

Transgenic Lines

Or-GAL4 or *Or-mCD8:GFP* lines have been previously described (Couto et al., 2005; Fishilevich and Vosshall, 2005; Komiyama et al., 2004), as have *pebbled-GAL4* (Sweeney et al., 2007), *UAS-mCD8:GFP* (Lee and Luo, 1999), and *10XUAS-IVS-mtdT* (Pfeiffer et al., 2010). See Supplemental Information for details on mutant alleles and additional transgenic lines.

Mosaic Analyses

hsFlp MARCM analyses were performed as previously described (Lee and Luo, 1999; Komiyama et al., 2004) with slight modifications. To analyze axon projections in adult brains using hsFlp MARCM, animals between 0-24h APF were heat shocked for 10 min at 37°C. For *pebbled-GAL4* hsFlp MARCM, newly formed pupae (0h APF animals) were heat-shocked for 5-10 min at 37°C and dissected at 24h APF.

Immunofluorescence

Tissue dissection and immunostaining were performed according to previously described methods (Sweeney et al., 2007). See Supplemental Information for antibody information. Confocal images were collected with a Zeiss LSM 510 and processed with Zeiss LSM software, ImageJ, and Adobe Photoshop.

See Supplemental Experimental Procedures for details on mutant alleles and transgenic lines, immunofluorescence and antibodies, quantification procedures, and genotypes for experiments described in main figures.

SUPPLEMENTAL INFORMATION

Supplemental Information includes Supplemental Experimental Procedures and seven figures and can be found with this article online at http://dx.doi.org/10.1016/j.neuron.2013.03.022.

ACKNOWLEDGMENTS

We thank Chris Potter for sharing unpublished *Orco-GAL80* transgenic flies, Alex Kolodkin and Zhuhao Wu for reagents and discussions, and Thomas Clandinin, Kang Shen, and members of the Luo lab for comments on the manuscript. W.J.J. was supported by the Stanford Neurosciences Graduate Program, the Kendall Fund, and an NIH NRSA Predoctoral Fellowship (5 F31 NS071697), and dedicates this work to A. Wittstruck. This work was supported by NIH grant R01-DC005982 (to L.L.). L.L. is an investigator at the Howard Hughes Medical Institute.

Accepted: March 20, 2013
Published: May 22, 2013

REFERENCES

Ayoob, J.C., Terman, J.R., and Kolodkin, A.L. (2006). *Drosophila* Plexin B is a Sema-2a receptor required for axon guidance. Development *133*, 2125–2135.

Carvalho, R.F., Beutler, M., Marler, K.J., Knöll, B., Becker-Barroso, E., Heintzmann, R., Ng, T., and Drescher, U. (2006). Silencing of EphA3 through a *cis* interaction with ephrinA5. Nat. Neurosci. *9*, 322–330.

Chou, Y.H., Zheng, X., Beachy, P.A., and Luo, L. (2010). Patterning axon targeting of olfactory receptor neurons by coupled hedgehog signaling at two distinct steps. Cell *142*, 954–966.

Couto, A., Alenius, M., and Dickson, B.J. (2005). Molecular, anatomical, and functional organization of the *Drosophila* olfactory system. Curr. Biol. *15*, 1535–1547.

Endo, K., Aoki, T., Yoda, Y., Kimura, K., and Hama, C. (2007). Notch signal organizes the *Drosophila* olfactory circuitry by diversifying the sensory neuronal lineages. Nat. Neurosci. *10*, 153–160.

Fishilevich, E., and Vosshall, L.B. (2005). Genetic and functional subdivision of the *Drosophila* antennal lobe. Curr. Biol. *15*, 1548–1553.

Haklai-Topper, L., Mlechkovich, G., Savariego, D., Gokhman, I., and Yaron, A. (2010). Cis interaction between Semaphorin6A and Plexin-A4 modulates the repulsive response to Sema6A. EMBO J. *29*, 2635–2645.

Hallem, E.A., and Carlson, J.R. (2006). Coding of odors by a receptor repertoire. Cell *125*, 143–160.

Hong, W., Zhu, H., Potter, C.J., Barsh, G., Kurusu, M., Zinn, K., and Luo, L. (2009). Leucine-rich repeat transmembrane proteins instruct discrete dendrite targeting in an olfactory map. Nat. Neurosci. *12*, 1542–1550.

Hong, W., Mosca, T.J., and Luo, L. (2012). Teneurins instruct synaptic partner matching in an olfactory map. Nature *484*, 201–207.

Hornberger, M.R., Dütting, D., Ciossek, T., Yamada, T., Handwerker, C., Lang, S., Weth, F., Huf, J., Wessel, R., Logan, C., et al. (1999). Modulation of EphA receptor function by coexpressed ephrinA ligands on retinal ganglion cell axons. Neuron *22*, 731–742.

Imai, T., Yamazaki, T., Kobayakawa, R., Kobayakawa, K., Abe, T., Suzuki, M., and Sakano, H. (2009). Pre-target axon sorting establishes the neural map topography. Science *325*, 585–590.

Jefferis, G.S.X.E., Marin, E.C., Stocker, R.F., and Luo, L. (2001). Target neuron prespecification in the olfactory map of *Drosophila*. Nature *414*, 204–208.

Jefferis, G.S., Vyas, R.M., Berdnik, D., Ramaekers, A., Stocker, R.F., Tanaka, N.K., Ito, K., and Luo, L. (2004). Developmental origin of wiring specificity in the olfactory system of *Drosophila*. Development *131*, 117–130.

Jefferis, G.S., Potter, C.J., Chan, A.M., Marin, E.C., Rohlfing, T., Maurer, C.R., Jr., and Luo, L. (2007). Comprehensive maps of *Drosophila* higher olfactory centers: spatially segregated fruit and pheromone representation. Cell *128*, 1187–1203.

Jukam, D., and Desplan, C. (2010). Binary fate decisions in differentiating neurons. Curr. Opin. Neurobiol. *20*, 6–13.

Kao, T.J., and Kania, A. (2011). Ephrin-mediated *cis*-attenuation of Eph receptor signaling is essential for spinal motor axon guidance. Neuron *71*, 76–91.

Kolodkin, A.L., and Tessier-Lavigne, M. (2011). Mechanisms and molecules of neuronal wiring: a primer. Cold Spring Harb. Perspect. Biol. *3*, a001727.

Komiyama, T., Carlson, J.R., and Luo, L. (2004). Olfactory receptor neuron axon targeting: intrinsic transcriptional control and hierarchical interactions. Nat. Neurosci. *7*, 819–825.

Komiyama, T., Sweeney, L.B., Schuldiner, O., Garcia, K.C., and Luo, L. (2007). Graded expression of semaphorin-1a cell-autonomously directs dendritic targeting of olfactory projection neurons. Cell *128*, 399–410.

Kovall, R.A. (2008). More complicated than it looks: assembly of Notch pathway transcription complexes. Oncogene *27*, 5099–5109.

Kuzina, I., Song, J.K., and Giniger, E. (2011). How Notch establishes longitudinal axon connections between successive segments of the *Drosophila* CNS. Development *138*, 1839–1849.

Langen, M., Koch, M., Yan, J., De Geest, N., Erfurth, M.L., Pfeiffer, B.D., Schmucker, D., Moreau, Y., and Hassan, B.A. (2013). Mutual inhibition among postmitotic neurons regulates robustness of brain wiring in *Drosophila*. eLife *2*, e00337.

Lattemann, M., Zierau, A., Schulte, C., Seidl, S., Kuhlmann, B., and Hummel, T. (2007). Semaphorin-1a controls receptor neuron-specific axonal convergence in the primary olfactory center of *Drosophila*. Neuron *53*, 169–184.

Lee, T., and Luo, L. (1999). Mosaic analysis with a repressible cell marker for studies of gene function in neuronal morphogenesis. Neuron *22*, 451–461.

Li, P., Collins, K.M., Koelle, M.R., and Shen, K. (2013). LIN-12/Notch signaling instructs postsynaptic muscle arm development by regulating UNC-40/DCC and MADD-2 in Caenorhabditis elegans. eLife *2*, e00378.

Louvi, A., and Artavanis-Tsakonas, S. (2006). Notch signalling in vertebrate neural development. Nat. Rev. Neurosci. *7*, 93–102.

Marquardt, T., Shirasaki, R., Ghosh, S., Andrews, S.E., Carter, N., Hunter, T., and Pfaff, S.L. (2005). Coexpressed EphA receptors and ephrin-A ligands mediate opposing actions on growth cone navigation from distinct membrane domains. Cell *121*, 127–139.

Pfeiffer, B.D., Ngo, T.T., Hibbard, K.L., Murphy, C., Jenett, A., Truman, J.W., and Rubin, G.M. (2010). Refinement of tools for targeted gene expression in *Drosophila*. Genetics *186*, 735–755.

Redmond, L., Oh, S.R., Hicks, C., Weinmaster, G., and Ghosh, A. (2000). Nuclear Notch1 signaling and the regulation of dendritic development. Nat. Neurosci. *3*, 30–40.

Sanes, J.R., and Yamagata, M. (2009). Many paths to synaptic specificity. Annu. Rev. Cell Dev. Biol. *25*, 161–195.

Sestan, N., Artavanis-Tsakonas, S., and Rakic, P. (1999). Contact-dependent inhibition of cortical neurite growth mediated by notch signaling. Science *286*, 741–746.

Silbering, A.F., Rytz, R., Grosjean, Y., Abuin, L., Ramdya, P., Jefferis, G.S., and Benton, R. (2011). Complementary function and integrated wiring of the evolutionarily distinct Drosophila olfactory subsystems. J. Neurosci. *31*, 13357–13375.

Stocker, R.F., Lienhard, M.C., Borst, A., and Fischbach, K.F. (1990). Neuronal architecture of the antennal lobe in *Drosophila melanogaster*. Cell Tissue Res. *262*, 9–34.

Sweeney, L.B., Couto, A., Chou, Y.H., Berdnik, D., Dickson, B.J., Luo, L., and Komiyama, T. (2007). Temporal target restriction of olfactory receptor neurons by Semaphorin-1a/PlexinA-mediated axon-axon interactions. Neuron *53*, 185–200.

Sweeney, L.B., Chou, Y.H., Wu, Z., Joo, W., Komiyama, T., Potter, C.J., Kolodkin, A.L., Garcia, K.C., and Luo, L. (2011). Secreted semaphorins from degenerating larval ORN axons direct adult projection neuron dendrite targeting. Neuron *72*, 734–747.

Wu, Z., Sweeney, L.B., Ayoob, J.C., Chak, K., Andreone, B.J., Ohyama, T., Kerr, R., Luo, L., Zlatic, M., and Kolodkin, A.L. (2011). A combinatorial semaphorin code instructs the initial steps of sensory circuit assembly in the *Drosophila* CNS. Neuron *70*, 281–298.

Yaron, A., and Sprinzak, D. (2012). The *cis* side of juxtacrine signaling: a new role in the development of the nervous system. Trends Neurosci. *35*, 230–239.

Neuron, Volume *78*
Supplemental Information

Linking Cell Fate, Trajectory Choice, and Target Selection: Genetic Analysis of Sema-2b in Olfactory Axon Targeting

William J. Joo, Lora B. Sweeney, Liang Liang, and Liqun Luo

Figure S1. Comprehensive Analysis of ORN Axon Targeting in *sema-2b*$^{-/-}$ Adults (Related to Figure 2).

(A) Loss of Sema-2b causes severe trajectory and glomerular targeting defects in seven additional ventromedial ORN classes. In all cases, a major proportion of axons aberrantly selects dorsolateral trajectories and mistargets to dorsolateral regions of the antennal lobe, whereas remaining axons retain ventral trajectories and terminate in approximately correct target regions.

(B) Five additional dorsolateral classes are largely unaffected in *sema-2b*$^{-/-}$ mutants. *Gr21a-GAL4* labels the CO_2-sensitive V glomerulus (ipsilateral only) and is the only ventral ORN class examined with normal trajectory and targeting in *sema-2b*$^{-/-}$ mutant brains (rightmost column).

(C) Four additional dorsomedial classes primarily exhibit only trajectory phenotypes in *sema-2b*$^{-/-}$ mutants. *AM29-GAL4* labels the dorsolateral DL4 glomerulus in addition to DM6 (third column); DM6 ORNs normally select ventromedial trajectories, but instead select dorsolateral trajectories in *sema-2b*$^{-/-}$ brains.

Genotypes: (top rows) *UAS-mCD8:GFP;; Or-GAL4/+*. (bottom rows) *UAS-mCD8:GFP; sema-2b*^{f02042}*/sema-2b*^{f02042}*; Or-GAL4/+*. For Or9a: Or9a-mCD8:GFP and *sema-2b*^{f02042}*, Or9a-mCD8:GFP/sema-2b*^{f02042}.

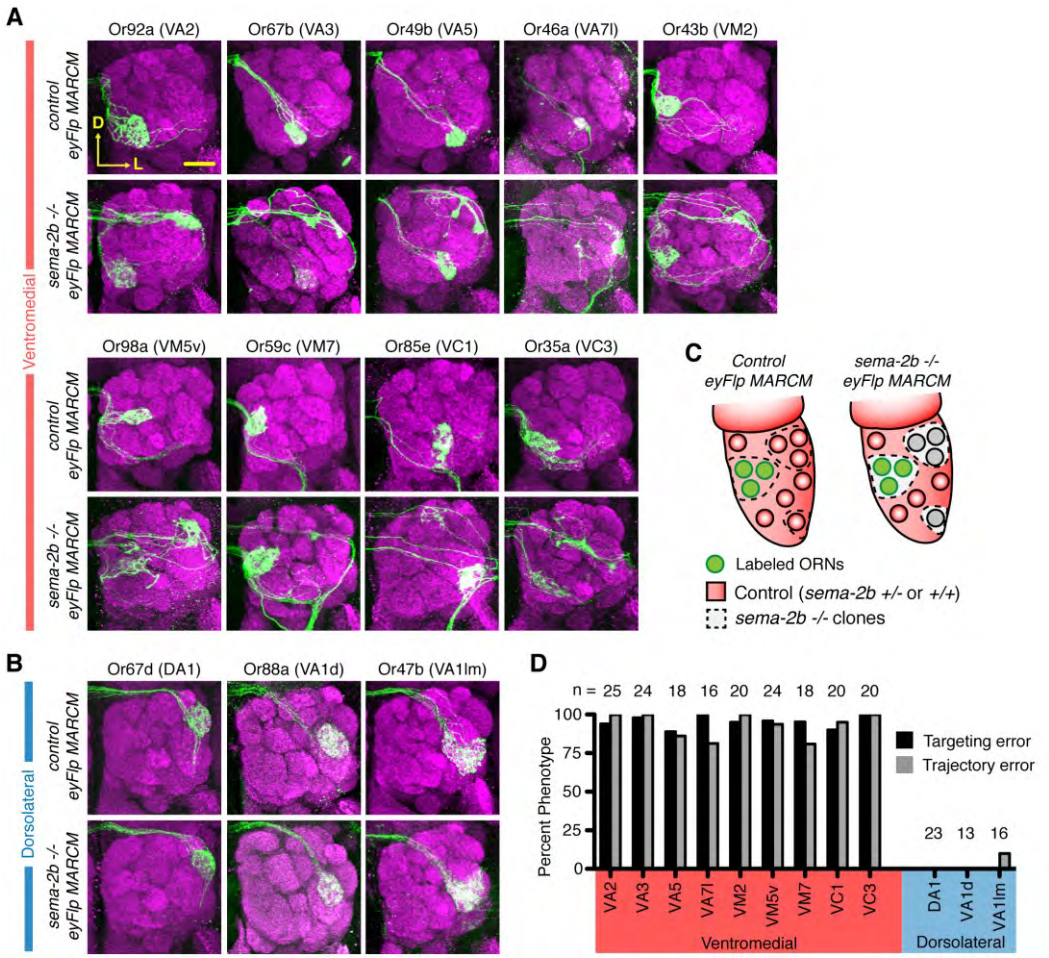

Figure S2. *sema-2b*$^{-/-}$ eyFlp MARCM Phenocopies Whole Animal Mutants (Related to Figure 2).

(A) Control (top) or *sema-2b*$^{-/-}$ (bottom) ORN clones generated by eyFlp-based MARCM and labeled with class-specific Or-GAL4 lines. In all nine ventromedial classes examined, *sema-2b*$^{-/-}$ mutant axons incorrectly choose dorsolateral trajectories and mistarget to dorsolateral regions of the antennal lobe.

(B) As expected based on whole animal mutant analyses, *sema-2b*$^{-/-}$ dorsolateral ORN axons exhibit normal trajectory and targeting patterns.

(C) Schematic of the eyFlp MARCM approach, in which *eyeless-Flp* drives mitotic recombination to create homozygous mutant clones selectively in ORNs. Left, in control eyFlp MARCM, all cells and thus all MARCM clones (dotted lines) are WT; Right, in *sema-2b*$^{-/-}$ eyFlp MARCM, all labeled ORNs (green) are *sema-2b*$^{-/-}$ (grey), but many *sema-2b*$^{-/-}$ ORNs are not labeled (grey but not green) because they do not express a particular Or-GAL4. Red are control (*sema-2b*$^{+/-}$ or *sema-2b*$^{+/+}$) cells.

(D) Quantification of eyFlp MARCM trajectory and targeting phenotypes for ventromedial and dorsolateral ORN classes; black, glomerular targeting error; gray, axon trajectory error; red, ventromedial classes; blue, dorsolateral classes.

Genotypes: (A-B, top) *UAS-mCD8:GFP, eyFlp, FRT19A/+; FRTG13/FRTG13, TubP-GAL80; Or-GAL4/+*. (A-B, bottom) *UAS-mCD8:GFP, eyFlp, FRT19A/+; FRTG13, sema-2b*^{f02042}*/FRTG13, TubP-GAL80; Or-GAL4/+*.

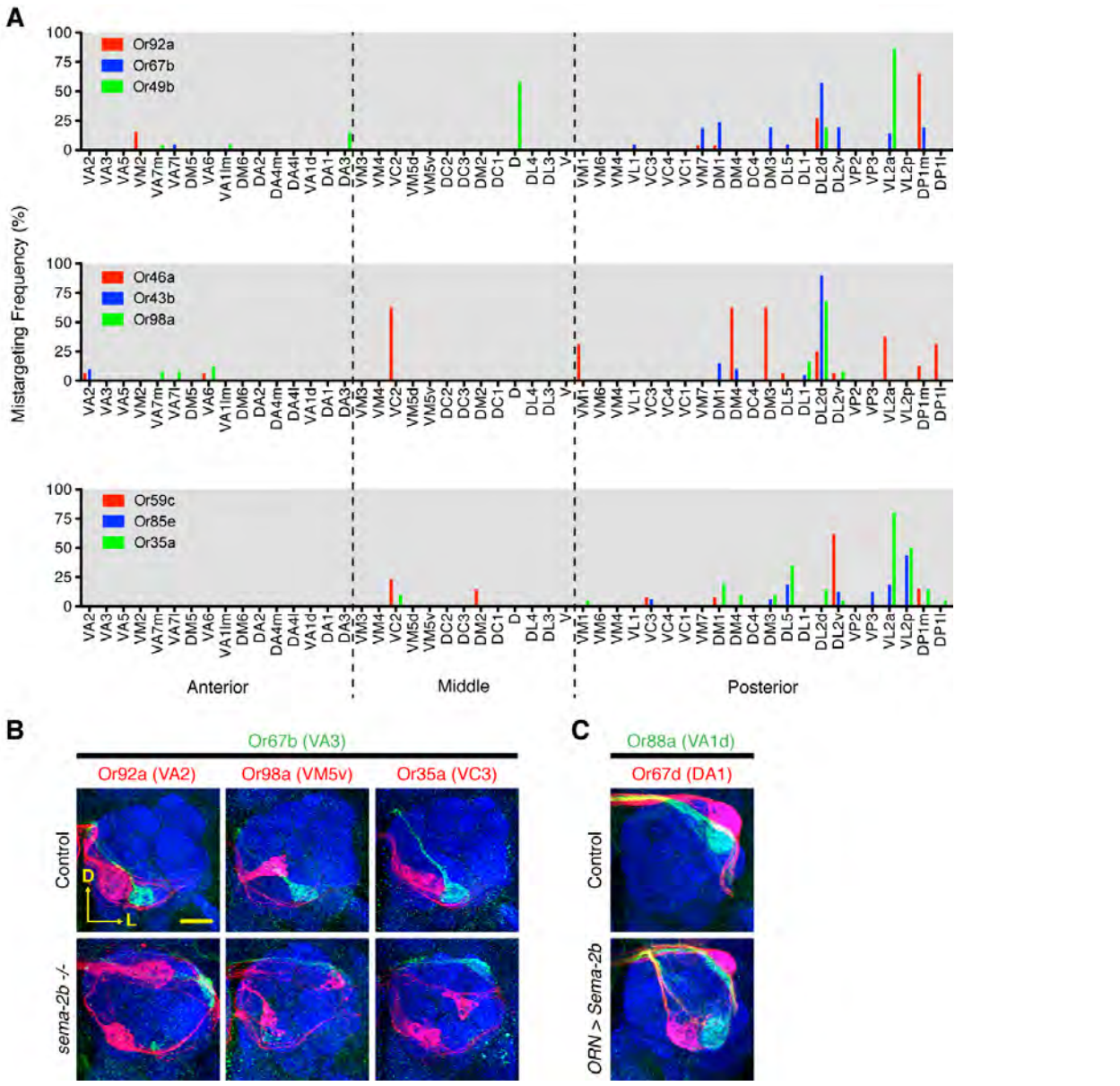

Figure S3. Mistargeting Specificity in Sema-2b Loss- and Gain-of Function Manipulations (Related to Figure 2).

(A) Frequency of glomerular mistargeting in *sema-2b*$^{-/-}$ eyFlp MARCM. Y axis, percentage of cases observed by hemisphere; X axis, antennal lobe glomeruli listed from ventromedial to dorsolateral and separated into anterior, middle, and posterior sections of the antennal lobe (as in Figure 2D). For clarity, data are shown in groups of three ORN classes. All classes primarily mistargeted to dorsolateral glomeruli in the posterior region of the antennal lobe. However, each ventromedial ORN class exhibited specific mistargeting patterns rather than randomly mistargeting to all dorsolateral glomeruli. For example, Or98a+ *sema-2b*$^{-/-}$ axons mistargeted most frequently to the DL2d glomerulus, whereas those of Or92a mistargeted most frequently to DP1m.

(B) Or67b ORN axons (green) co-labeled with Or92a, Or98a, or Or35a axons (red) in control (top) or *sema-2b*$^{-/-}$ mutant brains. Mistargeting Or67b axons most frequently project to the

dorsolateral corner of the antennal lobe, and do not intermingle with mistargeted axons of other ORN classes. Or92a axons mistarget medially but seldom contiguously with respect to Or67b axons (16/20=80% hemispheres). Or98a axons (34/40=85% hemispheres) mistarget medially and adjacently to Or67b axons, while Or35a axons mistarget ventromedially relative to Or67b (30/34=88% hemispheres). Genotypes: (B, top) *UAS-mtdT; sema-2b^{f02042}, Or67b-mCD8:GFP/CyO; Or-GAL4/+*. (B, bottom) *UAS-mtdT; sema-2b^{f02042}, Or67b-mCD8:GFP/sema-2b^{f02042}; Or-GAL4/+*.

(C) Or88a axons (green) co-labeled with Or67d axons (red) in control brains (top) project dorsolaterally to the adjacent VA1d and DA1 glomeruli, respectively. In brains with ORN-specific Sema-2b overexpression (bottom), both Or88a and Or67d axons exhibit ectopic ventromedial trajectories and mistarget to two adjacent ventromedial glomeruli (18/18=100% hemispheres). Mistargeting Or67d axons are medial to mistargeting Or88a axons in most cases (16/18=89% hemispheres). Genotypes: (top) *Or67d-QF, QUAS-mtdT-3xHA/Y; UAS-Sema-2b/+; Or88a-mCD8:GFP*. (bottom) *Or67d-QF, QUAS-mtdT-3xHA/pebbled-GAL4; UAS-Sema-2b/+; Or88a-mCD8:GFP*.

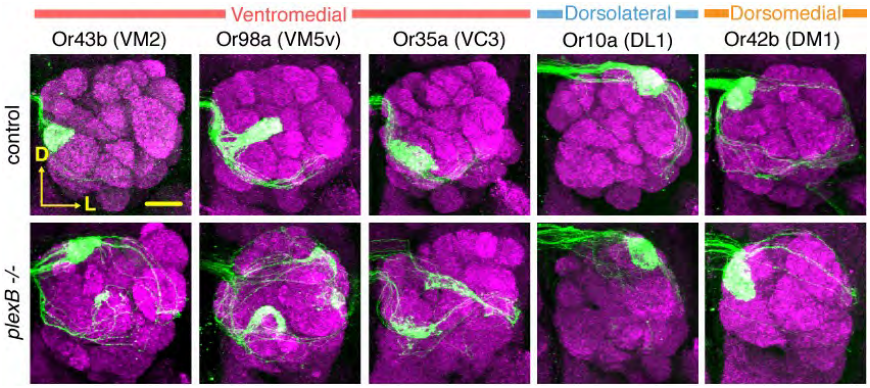

Figure S4. Analysis of Additional ORN Classes in *plexB$^{-/-}$* Mutants (Related to Figure 3).
Additional ORN classes in *plexB$^{-/-}$* mutant brains. Ventromedial ORN classes exhibit phenotypes strikingly similar to those of *sema-2b$^{-/-}$* mutants, with dorsolateral trajectories and mistargeting. Like Or67d ORNs (Figure 3C), dorsolateral Or10a ORNs are largely unaffected. Finally, dorsomedial Or42b ORNs exhibit trajectory defects only. Genotypes: *Or-GAL4, UAS-mCD8:GFP*; *plexB^{KG00878}/plexB^{KG00878}*. For Or22a: *Or22a-mCD8GFP/+; plexB^{KG00878}/plexB^{KG00878}*.

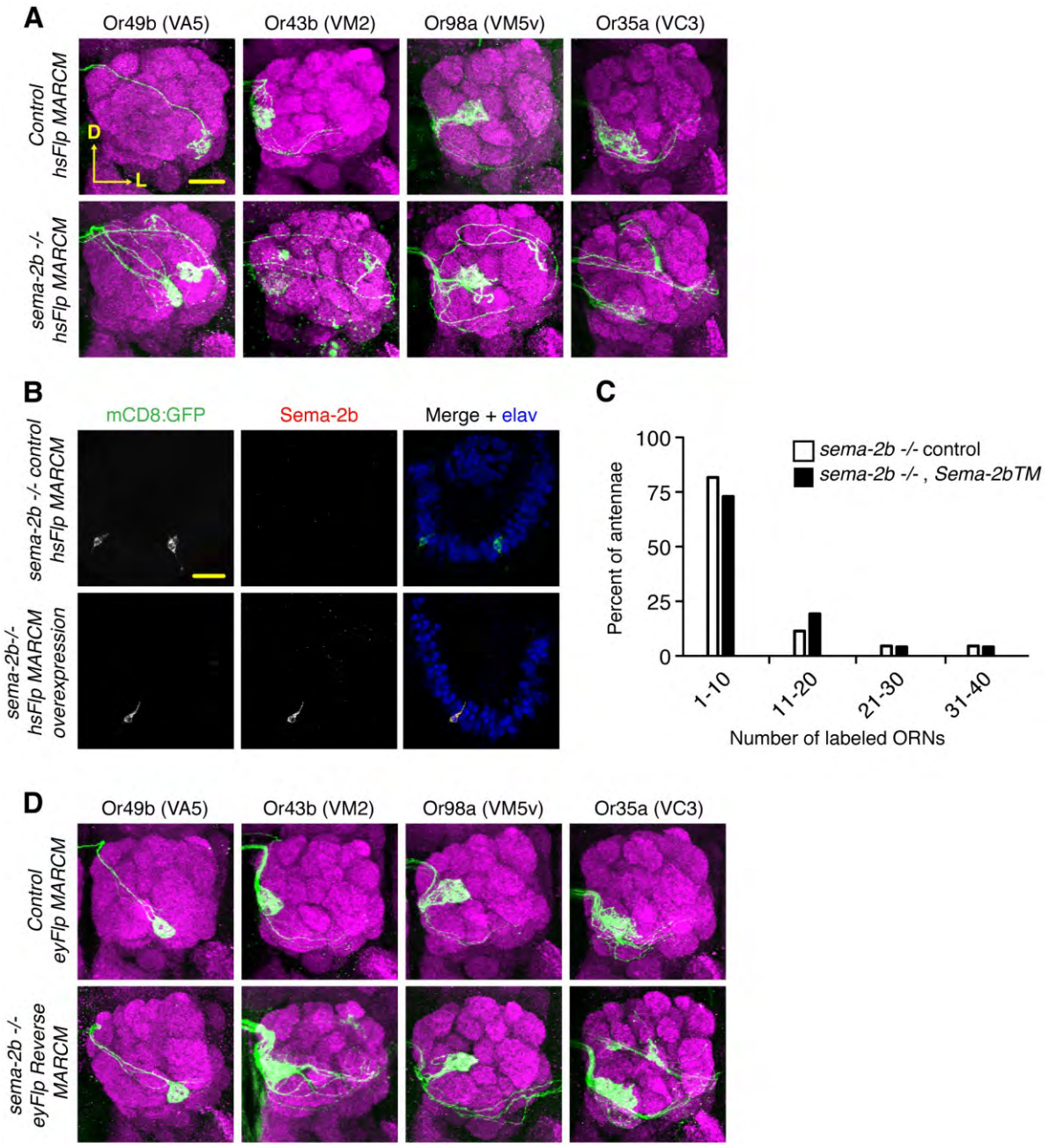

Figure S5. Additional Data for Mosaic Analysis of *sema-2b* (Related to Figure 4).
(A) *Or-GAL4*-driven mCD8:GFP labels axons of individual ventromedial ORN classes in control (top) and *sema-2b*$^{-/-}$ (bottom) hsFlp MARCM. As with Or92a and Or67b axons (Figure 6), *sema-2b*$^{-/-}$ axons of all examined ventromedial classes aberrantly choose dorsolateral trajectories and target dorsolateral glomeruli, with a fraction of axons retaining correct trajectory and targeting. Genotypes: (top) *hsFlp, UAS-mCD8:GFP/+; FRTG13/FRTG13, TubP-GAL80; Or-GAL4/+*. (bottom) *hsFlp, UAS-mCD8:GFP/+; FRTG13, sema-2b*^{f02042}*/FRTG13, TubP-GAL80; Or-GAL4/+*

(B) Examples of single antennae from *sema-2b*$^{-/-}$ mutants, in which *pebbled-GAL4* hsFlp MARCM generates control (top) or Sema-2b^{TM}-overexpressing (bottom) ORNs labeled with mCD8:GFP. To induce clones, 0h APF pupa were heat-shocked at 37°C for 5-10 minutes. Top, example antenna with three labeled ORNs. Bottom, example antenna with a single labeled ORN overexpressing Sema-2b^{TM}. Left, mCD8:GFP; middle, Sema-2b staining; right, overlay of left and middle panels together with Elav staining, which labels all neuronal nuclei. Scale bar = 20 μm.
(C) Quantification of *pebbled-GAL4* hsFlp MARCM labeling efficiency, based on the number of labeled ORNs per antenna. On average, each antennae contained ~10 labeled ORNs, representing < 1% of the ~1,300 ORNs per antenna. Respective n (antennae) = 44 (*sema-2b*$^{-/-}$ *control*) and 24 (*sema-2b*$^{-/-}$*, UAS-sema-2b*^{TM}).
(D) *Or-GAL4*-driven mCD8:GFP labels axons of individual ventromedial ORN classes in control (top) and *sema-2b*$^{-/-}$ reverse (bottom) eyFlp MARCM. In the presence of *sema-2b*$^{-/-}$ background clones (see Figure 4G), WT Or43b and Or35a axons exhibit dorsolateral trajectory and targeting phenotypes much like *sema-2b*$^{-/-}$ axons. In contrast, Or49b and Or98a axons remain largely normal.

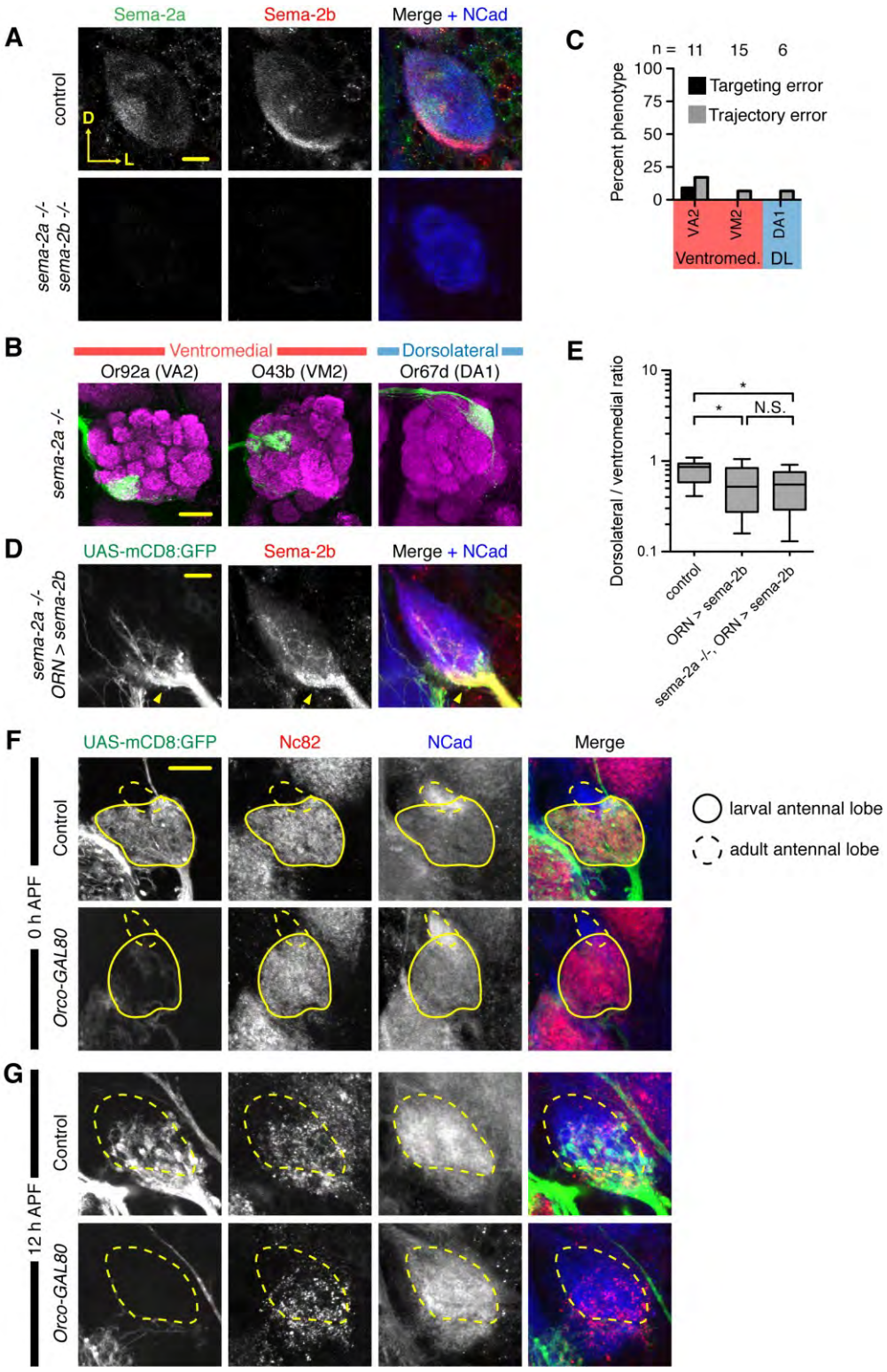

Figure S6. *sema-2a* mutant phenotypes and Orco-GAL80 function (Related to Figure 5).

(A) Overlapping Sema-2a and Sema-2b expression patterns at 24h APF. Like Sema-2b, Sema-2a is enriched within the ventromedial antennal lobe (top). Sema-2a and Sema-2b staining is absent in *sema-2a*$^{-/-}$*, sema-2b*$^{-/-}$ double mutant brains (bottom). Scale bar = 10 μm.
(B) Glomerular targeting of axons (labeled in green) from specific ORN classes in *sema-2a*$^{-/-}$ mutant adult brains. Or92a, Or43b, and Or67d axons do not exhibit significant trajectory or targeting phenotypes. Scale bar = 20 μm.
(C) Quantification of *sema-2a*$^{-/-}$ adult mutant phenotypes for two ventromedial and a dorsolateral ORN classes.
(D) ORN-specific overexpression of Sema-2b in a *sema-2a*$^{-/-}$ mutant background at 29°C biases axon trajectories ventromedially, just as in Sema-2b overexpression in a *WT* background (Figure 1F). Scale bar = 10 μm. Genotype: *pebbled-GAL4/+; sema-2a*^{P2}*, UAS-mCD8:GFP/sema-2a*^{P2}*; UAS-sema-2b/+*
(E) Quantification of dorsolateral/ventromedial axon bundle ratio, labeled as in Figure 1. For *sema-2a*$^{-/-}$*, ORN > sema-2b*, mean ratio = .53, n = 16. 29°C control and ORN > Sema-2b overexpression data from Figure 1 are shown for comparison. * $p < 0.05$, one-way ANOVA with Bonferroni's Multiple Comparison Test.
(F) At 0h APF, *pebbled-GAL4*-driven *UAS-mCD8:GFP* labels larval ORNs, which arborize within the nc82+ and weakly NCad+ larval antennal lobe (solid outline). Strong NCad immunostaining labels the developing adult antennal lobe (dotted outline). *Orco-GAL80* can efficiently suppress *pebbled-GAL4*, as evidenced by almost complete suppression of *UAS-mCD8:GFP* within the larval antennal lobe (bottom row). Scale bar = 20 μm.
(G) By 12h APF, the adult antennal lobe expands concurrently with larval ORN degeneration. nc82 staining labels the regressing larval antennal lobe. As in 0h APF pupae, *Orco-GAL80* effectively suppresses *pebbled-GAL4* in larval ORNs. Pioneering axons from adult ORNs will reach the adult antennal lobe roughly six hours later. Scale bar = 20 μm.
Genotype: (A-B, top rows) *pebbled-GAL4/+; UAS-mCD8:GFP/+*. (A-B, bottom rows) *pebbled-GAL4/+; UAS-mCD8:GFP/Orco-GAL80.*

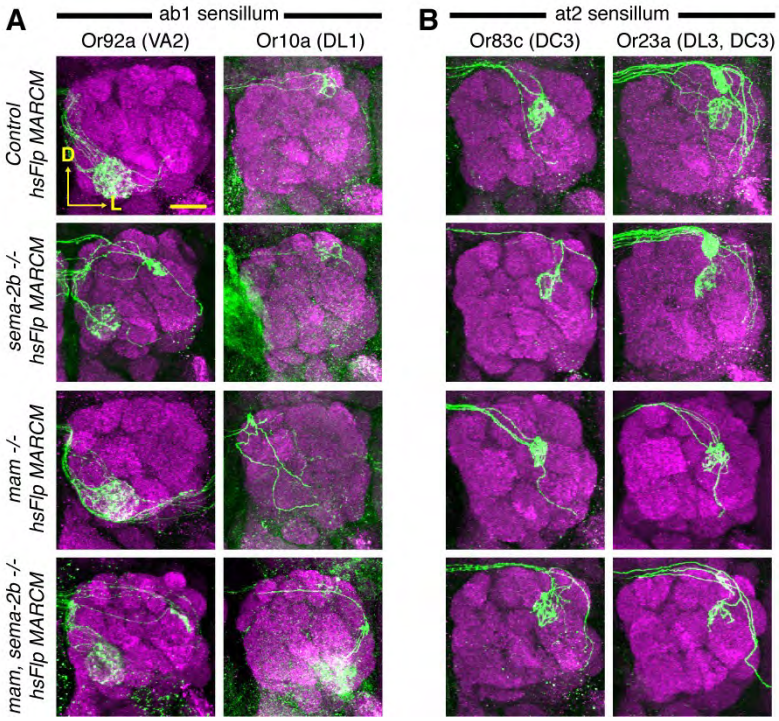

Figure S7. *sema-2b* Is Epistatic to *mastermind* In Two Additional Pairs of ORN Classes (Related to Figure 6).

(A) hsFlp MARCM for Or10a (left column) and Or92a (right column) ORNs; both reside within the ab1 sensillum and derive from a common ORN precursor cell. According to a previous study (Endo et al., 2007), Or92a ORNs are Notch-OFF whereas Or10a ORNs are Notch-ON. *mam*$^{-/-}$ Or92a axons target normally to the VA2 glomerulus (18/18 clones), consistent with their previously described Notch-OFF status. *mam*$^{-/-}$, *sema-2b*$^{-/-}$ double mutant Or92a axons project and mistarget dorsolaterally (18/25=72% clones), thus phenocopying *sema-2b*$^{-/-}$ single mutant axons (second and fourth rows). Or10a axons behave in a complementary fashion. *sema-2b*$^{-/-}$ Or10a axons remain unaffected, (10/10 clones) while *mam*$^{-/-}$ axons take ventromedial trajectories and mistarget to the VA2 glomerulus (8/8 clones). In *mam*$^{-/-}$, *sema-2b*$^{-/-}$ double mutant clones, Or10a axons revert to a dorsolateral trajectory (9/9 clones), although DL1 targeting is only partially rescued (3/9 = 33% clones).

(B) hsFlp MARCM for Or83c (left column) and Or23a (right column) ORNs , which co-reside in the at2 sensillum. Or83c axons normally take a more medial trajectory to the DC3 glomerulus, but switch to a dorsolateral trajectory in *sema-2b*$^{-/-}$ MARCM (17/20=85% clones). As with Or92a, *mam*$^{-/-}$ Or83c axons are normal (20/20 clones), and *mam*$^{-/-}$, *sema-2b*$^{-/-}$ double mutant axons phenocopy *sema-2b*$^{-/-}$ single mutant axons (18/22=82% clones). The *Or23a-GAL4* line # 17.2 co-labels both ORN classes in the at2 sensillum; their axons take medial and lateral trajectories to DC3 and DL3, respectively. All *sema-2b*$^{-/-}$ Or23a axons choose dorsolateral trajectories as expected from the both Or83c phenotype and the dorsolateral location of DL3. In *mam*$^{-/-}$ clones, all axons switched to medial trajectories and targeted DC3 (12/12 clones). Interestingly, in *mam*$^{-/-}$, *sema-2b*$^{-/-}$ double mutant clones, axons reverted to dorsolateral

trajectories (15/18 clones=83%). Thus, in both Or92a/10a and Or83c/Or23a pairs, *sema-2b* is epistatic to *mam* and mediates trajectory selection downstream of Notch signaling, just as in the ORN pair labeled by *AM29-GAL4* (Figure 6).

Supplemental Experimental Procedures

Mutant Alleles and Transgenic Lines

Loss of function experiments used the following mutant alleles: *sema-2b*^{f02042}, a pBac insertion (Thibault et al., 2004); *sema-2a*^{P2}, a P-element insertion (Ayoob et al., 2006); *plexB*^{KG00878}, a P-element insertion (Ayoob et al., 2006). Rescue and overexpression experiments utilized *UAS-plexB* (Ayoob et al., 2006), and *UAS-Sema-2b*^{TM} (Wu et al., 2011). UAS-Sema-2b was generated as follows: Sema-2b coding and 3'UTR regions were excised by digestion from *Drosophila* Genomic Resource Center cDNA clone pOT2-IP13724 with EcoRI and XhoI, ligated into a pUAST vector, and sequence-verified. Two transgenic lines were obtained on the 2nd and 3rd chromosomes, with comparable overexpression levels. For the *Orco-GAL80* line, the *GAL4-VP16* cassette from *pCasper4-Orco-GAL4-VP16* (Galindo and Smith, 2001) was excised by digestion with XbaI and NheI. The GAL80 coding sequence was PCR amplified from *pCasper4-GAL80* (C.J. Potter, unpublished) to include 5' XbaI, NotI and 3' XbaI restriction sites, and ligated into the digested pCasper4-Orco vector. The construct was sequence verified.

Immunofluorescence and Antibodies

The following antibodies were used according to previous methods (Sweeney et al., 2007): Mouse nc82 [1:35; Developmental Studies Hybridoma Bank, (DSHB)], rat anti-DNcad (DN-Ex #8; 1:40; DSHB), mouse anti-Elav (9F8A9; 1:100; DSHB), rat anti-mCD8a (CT-CD8a; 1:100; Invitrogen/CALTAG), chicken anti-GFP (1:1000; Aves Labs), rabbit anti-Sema-2b (Sweeney et al., 2011). Secondary antibodies were raised in goat or donkey against rabbit, mouse, rat and chicken antisera (Jackson Immunoresearch), conjugated to Alexa 488, FITC, Cy3, Cy5, or Alexa 647.

Quantification Procedures

For axon bundle quantifications, the medial-most 5-10 sections (5-10 microns) of each confocal stack were collapsed into maximum intensity Z-projections. Within such partial projections, the respective two-dimensional areas (μm^2) of the dorsolateral and ventromedial axon bundles, visualized by the membrane marker mCD8:GFP, were calculated using Zeiss LSM software. Finally, these values were divided for an estimate of dorsolateral/ventromedial axon bundle ratio.

Sema-2b fluorescence intensity was quantified from identical Z-projections as above using ImageJ. Ventromedial and dorsolateral axon bundles were outlined as regions of interest and Sema-2b fluorescence/pixel quantified relative to mCD8:GFP fluorescence/pixel for each bundle.

For phenotype penetrance quantifications in adult brains, trajectory error was scored per antennal lobe while targeting error was scored per brain. Mistargeting frequency was calculated as (hemispheres with mistargeting to glomerulus)/(total brains hemispheres with mistargeting).

For axon trajectory quantifications in *pebbled-GAL4* hsFlp MARCM, all samples with labeled axons were scored blind to genotypes.

Genotypes for Experiments Described in Main Figures

Figure 1 (B) *pebbled-GAL4/+; sema-2b^{f02042}, UAS-mCD8:GFP/sema-2b^{f02042}* (C) *pebbled-GAL4/+; sema-2b^{f02042}, UAS-mCD8:GFP/sema-2b^{f02042}; UAS-sema-2b/+*. (D) *pebbled-GAL4/+; sema-2b^{f02042}, UAS-mCD8:GFP/sema-2b^{f02042}, UAS-sema-2b^{TM}*. (F-G) *pebbled-GAL4/+; UAS-mCD8:GFP, UAS-sema-2b^{TM}/+*.

Figure 2. (A-C) *UAS-mCD8:GFP; sema-2b^{f02042}/sema-2b^{f02042}; Or-GAL4/+*.

Figure 3. (A) (top) *pebbled-GAL4, UAS-mtdT*. (middle) *pebbled-GAL4, UAS-mtdT;;; plexB^{KG00878}/plexB^{KG00878}*. (bottom) *pebbled-GAL4, UAS-mtdT; UAS-plexB/+;; plexB^{KG00878}/plexB^{KG00878}*. (C) *Or-GAL4, UAS-mCD8:GFP*/+; *plexB^{KG00878}/plexB^{KG00878}*

Figure 4. (B) (top) *hsFlp, UAS-mCD8:GFP/+; FRTG13/FRTG13, TubP-GAL80; Or-GAL4/+*. (bottom) *hsFlp, UAS-mCD8:GFP/+; FRTG13, sema-2b^{f02042}/FRTG13, TubP-GAL80; Or-GAL4/+*. (E) (top) *hsFlp, UAS-mCD8:GFP/pebbled-GAL4; FRT40a, sema-2b^{f02042}/FRT40a, tubP-GAL80, sema-2b^{f02042}*. (bottom) *hsFlp, UAS-mCD8:GFP/pebbled-GAL4; FRT40a, sema-2b^{f02042}, UAS-sema-2b^{TM}/FRT40a, tubP-GAL80, sema-2b^{f02042}*. (H) (top) *UAS-mCD8:GFP, eyFlp, FRT19A/+; FRTG13/FRTG13, TubP-GAL80; Or-GAL4/+*. (bottom) *UAS-mCD8:GFP, eyFlp, FRT19A/+; FRTG13/FRTG13, TubP-GAL80, sema-2b^{f02042}; Or-GAL4/+*.

Figure 5. (A) *pebbled-GAL4; sema2a^{P2}, sema2b^{f02042}, Orco-GAL80/sema-2a^{P2}, sema-2b^{f02042}, UAS-mCD8:GFP*. (C) *pebbled-GAL4; sema2a^{P2}, sema2b^{f02042}, Orco-GAL80/sema-2a^{P2}, sema-2b^{f02042}, UAS-mCD8:GFP; UAS-sema-2b/+*

Figure 6. (A) Genotype: *hsFlp, UAS-mCD8:GFP/+; AM29-GAL4, FRTG13, UAS-mCD8:GFP/FRTG13, TubP-GAL80.* (B) *hsFlp, UAS-mCD8:GFP/+; AM29-GAL4, FRTG13, sema-2b^{f02042}/FRTG13, TubP-GAL80.* (C) *hsFlp, UAS-mCD8:GFP/+; AM29-GAL4, FRTG13, mam^{k1514},UAS-mCD8:GFP/FRTG13, TubP-GAL80.* (D) *hsFlp, UAS-mCD8:GFP/+; AM29-GAL4, FRTG13, mam^{k1514}, sema-2b^{f02042}/FRTG13, TubP-GAL80.*

Supplemental References

Galindo, K., and Smith, D.P. (2001). A large family of divergent Drosophila odorant-binding proteins expressed in gustatory and olfactory sensilla. Genetics *159*, 1059–1072.

Thibault, S.T., Singer, M.A., Miyazaki, W.Y., Milash, B., Dompe, N.A., Singh, C.M., Buchholz, R., Demsky, M., Fawcett, R., Francis-Lang, H.L., et al. (2004). A complementary transposon tool kit for Drosophila melanogaster using P and piggyBac. Nat. Genet. *36*, 283–287.